

A new stratigraphic trap for CO₂ in the UK North Sea: appraisal using legacy information

Mark Wilkinson,

School of GeoSciences,

The University of Edinburgh,

Grant Institute,

The King's Buildings,

West Mains Road,

Edinburgh, UK

Phone +(0)131 650 5943

Fax +(0)131 668 3184

e-mail: mark.wilkinson@ed.ac.uk

A new stratigraphic trap for CO₂ in the UK North Sea: appraisal using legacy information

Mark Wilkinson^{a,d}, R. Stuart Haszeldine^{a,d}, Eric Mackay^{b,d}, Kevin Smith^{c,d} and Susanne Sargeant^{c,d}

^a School of GeoSciences, The University of Edinburgh, Grant Institute, The King's Buildings, West Mains Road, Edinburgh EH9 3JW

^b Institute of Petroleum Engineering, Heriot-Watt University, Riccarton Campus, Edinburgh, EH14 4AS

^c British Geological Survey, Murchison House, West Mains Road, Edinburgh EH9 3LA.

^d Scottish Carbon Capture and Storage

Corresponding author: mark.wilkinson@ed.ac.uk

Abstract

Using legacy information to search for geological CO₂ storage within saline aquifers is likely to be a cost-effective technique for commercial CCS projects. Here, a potential storage site was discovered, away from hydrocarbon reservoirs, using public information. CO₂ would be injected 15 – 40 km downdip from the margin of almost un-drilled

regionally extensive Permian (Rotliegend) Sandstone saline aquifer. The CO₂ would migrate buoyantly towards the aquifer margin under an evaporite top-seal, becoming partly trapped by residual saturation effects. Any remaining CO₂ would be retained in the stratigraphic pinchout trap at the edge of the aquifer. The lateral seal at the margin is most likely to be metamorphic basement – of presumed low permeability, inferred to be overlain by dolomite-anhydrite sediments. Using conservative assumptions, 170 – 690 Mt of CO₂ could be stored along a 50 km long section of the 300km margin of the reservoir. Preliminary modelling shows that 100 % of the CO₂ will be retained within the reservoir for at least 10,000 years. This demonstrates how small datasets, widely spread, can be adequate for a first stage investigation, and geological uncertainties can be identified for subsequent investigation.

Keywords: CO₂ storage, North Sea, Rotliegend, Zechstein, stratigraphic trap, residual saturation, legacy data

1. Introduction

Geological storage of CO₂ requires the identification of suitable strata and also suitable injection sites that utilise the strata. While there is abundant experience within the hydrocarbon industry at locating hydrocarbon accumulations, there is currently only limited experience in identifying and locating sites suitable for CO₂ storage beyond the regional scale, especially for saline aquifers. Some recent studies do focus on aquifers

and on the work-flows required for appraisal, (e.g. Carneiro et al., 2011; Hatzignatiou et al., 2011; Ogawa et al., 2011; Smith et al., 2011; Zhou et al, 2011) though most do not identify individual injection sites. Typical challenges associated with the early stages of appraisal of an aquifer storage site include:

- Acquisition of data for low cost
- Utilisation of small data sets, which are (much) less than modern technical requirements
- Thinly spread information across wide areas,
- Robust identification of promising settings,
- Exclusion of poor regions from further investigation,
- Identification of important geological uncertainties
- Target subsequent investigations, to improve confidence.

By analogy with the hydrocarbon industry, it might be presumed that most injection sites would utilise structural traps within the aquifers, which are analogues of hydrocarbon traps, such as anticlines and fault blocks. In this case, the trap retains the buoyant CO₂, while the surrounding aquifer allows for the dissipation of pressure away from the injection boreholes. However, there is another category of trap, the stratigraphic trap, which lacks a structure and relies on a lateral change in the reservoir rock, either a facies change to a seal lithology, or a lateral pinch out below an unconformity. Stratigraphic traps are more difficult to find and prove than structural traps using conventional hydrocarbon exploration techniques, which rely heavily on seismic surveying. The extent to which stratigraphic traps offer CO₂ storage potential is unknown, however such traps

might offer significant storage in some locations, especially perhaps in relatively young sediments where conventional structural traps are not developed. This paper describes a case study in which a stratigraphic trap, combined with residual saturation during CO₂ migration (IPCC, 2005), was identified as a promising storage scenario.

An area of the UK North Sea, centred on UK quadrants 28 and 29 (approximately 122 by 112 km; Fig 1) was studied with the aim of locating a site suitable for the storage of CO₂. The study area, defined by the project sponsors, lies approximately due east of the Midland Valley of Scotland, which is a major centre for CO₂ production in the UK. The area lies outside the area of the North Sea that has proved to be productive for hydrocarbons, and as such only a limited number of boreholes have been drilled. This is both an advantage for CO₂ storage in that there are few old boreholes to act as potential conduits for leakage to the surface, but a disadvantage in that there is limited subsurface information. The available quantity of cored rock sample was very limited, and the area has been relatively neglected in the literature in favour of the better-known hydrocarbon-rich areas. However, the regional stratigraphy of the area is known (Fig. 2) and there are published summaries of the regional geology (e.g. Gatliff et al., 1994) and maps (Stoker and Johnson, 1986). We have assessed the viability of this storage location using publicly available data, and information derived from well cores that are held by the British Geological Survey, which are available for viewing by interested parties.

The aim of the study was to survey the area, as a scoping exercise, to assess whether further investment should be made in more detailed work that would potentially include

the purchase of legacy seismic data for the identification of a storage site, and eventually the drilling of a test borehole. This study did not have access to seismic data, though (confidential) regional depth maps of key surfaces, derived from seismic, were made available by the project partners. There were two fundamental stages in the work: first to choose a suitable target reservoir-seal combination, and second to locate within this reservoir a suitable site for injection. In this context, the site location need only be general, for example within an identified portion of the area which displays promising geological characteristics. It was not expected that the study would achieve the level of detail that would eventually be required to locate a test borehole or future CO₂ injection facilities. No attempt was made here to assess factors such as economics, regulatory or public perception issues, and these remained to be addressed at a later stage of project development.

2. Methods

The regional geology of the area was studied from published sources. Regional maps of depth of potential reservoirs were constructed from depth contours for Quadrants 28 and 29 from Stoker and Johnson (1986), supplemented with borehole logs that are released by the UK Government. The criteria for assessing the suitability of a reservoir were primarily porosity and permeability; regional extent, depth of burial; and simple internal geology. Potential seals were assessed according to their lithology, thickness and regional extent. Strata were assessed in the following age / lithostratigraphic categories: Paleogene and Neogene; Upper Cretaceous Chalk; Lower Cretaceous; Triassic and Jurassic;

Permian Zechstein Evaporites; Permian Zechstein Carbonates; Permian Marl Slate / Kupferschiefer; Permian Rotliegend Group; Carboniferous and Devonian systems.

On the basis of the preliminary assessment (see section 3), core samples of both the Rotliegend Group and the underlying strata were examined and described, primarily to identify the sedimentary facies, allowing assessment of heterogeneity and likely reservoir quality of the sediments. Rotliegend core were available from only two boreholes within the study area, 29/25-1 and 28/12-1 (Fig. 3). A survey of the occurrence of volcanic rocks of Permian age within the region was undertaken, as they could be porosity-free intervals within the reservoir volume.

The storage capacity of the selected reservoir was assessed. For the calculation, the density of CO₂ is required, under storage conditions of pressure and temperature. There are no measured pore fluid pressure data known from within or close to the proposed storage area. Hence, pressures have had to be estimated using mud weights from boreholes, i.e. the pressure at the bottom of the borehole is calculated from the density of the drilling 'mud' within the borehole during drilling, and the borehole depth. This method has the disadvantage that the drilling mud must always be more highly pressured than the pore fluids to prevent a blow out, and so provides only a maximum limit to formation pore pressures. It has been assumed that the true pore fluid pressure of the reservoir is 90 % of the calculated pressure. CO₂ density was calculated using the on-line calculator of Duan et al. (1992), assuming 100 % purity. To assess the possibility that seismological activity could contribute to an unplanned release of CO₂, a survey of

seismicity data was undertaken using the British Geological Survey earthquake database, along with a description of neotectonics in the area.

From the results of the work above, a possible site for CO₂ injection was chosen, and preliminary modelling of injection undertaken using the STARS modelling package from the Computer Modelling Group Ltd. The modelled cross-section, derived from confidential depth maps of key surfaces supplied by the project partners, is shown in Fig. 4, and the location on Fig. 3. The cross-section is drawn using pessimistic assumptions where there are geological uncertainties, so that the transition from high quality seal halite to poorer quality seal dolomite / anhydrite in the Zechstein seal on the paleo-shelf to the SW is shown as far to the NE as is deemed likely (see section 4.2), and the extent of the underlying Rotliegend reservoir sandstone is given the minimum likely extent in a SW direction (see section 4.1). Even with this pessimistic reconstruction, an injection site can be proposed 15 km from the SW pinch-out of the reservoir, which coincides with the halite to dolomite / anhydrite lateral transition in the seal. For the numerical injection simulation, the cross-section of the model is assumed to be constant in a strike direction. The modelled volume is 60 km by 50 km by 3048 m (10,000 ft) depth represented by 24 by 20 by 20 grid blocks. Rock properties are in Table 1, assumed to be constant within each unit. The ratio of vertical to horizontal permeability has been assumed to be 0.1. Injection was assumed to be 5M tonnes CO₂ per year for 20 years into a single vertical borehole, set centrally in the strike direction. The model simulated both free-phase CO₂ as a supercritical fluid, and CO₂ in solution within the porewaters. Irreducible gas saturation is set to 0.05 in the basecase model, and the sensitivity of the results to the

value of this parameter were tested up to a value of 0.2. The model was run for 10,000 years after the end of injection.

3. Results

Table 2 summarises the regional assessment of potential storage units and seals in the study area. On the basis of this assessment, the Permian-age Rotliegend Sandstone Formation was identified as the most promising CO₂ storage unit, with the Upper Permian Zechstein evaporites as a seal. The remainder of the study was focussed on this reservoir-seal combination.

Table 3 summarises the distribution of Rotliegend sediments in legacy boreholes from hydrocarbon exploration, locations are on Fig. 3. Fig. 3 also shows the depth contours of the top Rotliegend surface from Stoker & Johnson (1986) for Quadrants 28 and 29, extrapolated into adjacent areas using borehole data (Table 3). The Rotliegend varies systematically in thickness and depth of burial, from 10 to 12 km burial depth in the NE (estimated from seismic mapping made available by the project partners, there are no borehole penetrations at such depths) to approximately 2 km in the SW of the area (Stoker & Johnson, 1986; Fig. 3). Thickness varies from >525m in borehole 29/18-1 (Glennie et al., 2003) to 0 m in the SW of the area, with a relatively limited number of boreholes that pass all the way through the formation, and hence measure the thickness. The Rotliegend storage unit thins to the southwest, though the exact edge is difficult to

define due to the small number of boreholes in the area. In Fig. 3 the limit of the Rotliegend is shown from Gatliff et al. (1994) and Stewart and Clark (1999). Here, the point at which the Rotliegend reservoir thins to zero thickness is referred to as the ‘pinch-out’, the nature of which is discussed in section 4.1.

Within the Zechstein seal, there is a lateral facies change from halite-dominated in the north, to more marginal dolomite and anhydrite in the south of the area. The exact location of the limit of the halite is uncertain, as there is only some agreement between Glennie et al. (2003) and Stewart and Clark (1999). Halokinesis has only occurred in the thicker halite in the north of the area (Stewart and Clark, 1999) so that there is a zone of between the southern limit of the halite, and the edge of the Rotliegend reservoir (Fig. 3) which was deemed to be the optimum location for CO₂ injection (Fig. 3) as having both a high probability of occurrence of both a reservoir and a reliable seal.

In borehole 29/25-1 there are two cored intervals. The upper cored interval (2682 - 2713 m driller’s depth), which is close to the top of the Rotliegend reservoir, is uniform red-brown low angle laminated sands with some low angle rippling (Fig. 5). The sands are only moderately sorted and have visible porosity, but no systematic variation in grain size within the cored interval. The lamination is due to mm-scale variations in grain size, in the fine - medium grain size range. There is minor bleaching associated with (what appear to be) high-angle natural fractures (Fig. 5).

The lower cored interval (3101 – 3106 m driller’s depth) is close to the base of the Rotliegend. The base is a pale matrix-supported pebble conglomerate with rounded clasts of sandstone and quartzite. This grades up into a pale granule sand with clasts which include a pale grey fine-grained igneous rock. This in turn is overlain by a similar pale-grey, phenocryst-rich fine-grained igneous rock. The top of the igneous interval is not cored, and the base coincides with a break in the core so that neither the upper nor the lower contacts are available for inspection. The borehole log indicates that the core should include the ‘Saalian Unconformity’ between the Devonian and the Rotliegend; however, this is not readily apparent in the core. In borehole 28/12-1, both low angle laminated sands and higher angle cross-bedded sands are present. Sorting is generally only moderate, though there is no matrix. There are no shale intervals or other potential barriers to vertical fluid flow.

The results of the modelling are shown as the distribution of supercritical and dissolved CO₂ (Fig. 6) at 10000 years after the end of injection. No free phase CO₂ escapes from the Rotliegend Sandstone reservoir in any of the modelled scenarios. During and after injection, the CO₂ gas migrates away from the borehole as a result of the dip of the top of the Rotliegend. The free-phase CO₂ reaches the pinch-out of the Rotliegend after around 500 years after the cessation of injection. The CO₂ then spreads laterally in an along-strike direction. Increasing the irreducible gas saturation reduced the mobility of the free-phase CO₂ due to increased residual saturation trapping.

4. Discussion

These initial estimates of total CO₂ storage potential in the reservoir and especially the dynamic modelling of injection, are very promising. However that means that additional work now has to be done on the way towards a licence application for CO₂ storage.

4.1. Reservoir

Aeolian sands that are lateral equivalents to the Rotliegend Sandstone within the study area form excellent and extensive hydrocarbon reservoirs in the North Sea. The majority of the UK's gas is extracted from these reservoirs, and there are 3 relatively small oil fields located close to the study area which include Rotliegend reservoirs (Heward et al., 2003; Fig. 3). However, given the very poor well coverage, there are inevitably uncertainties about the reservoir geology within the study area. The Rotliegend Sandstone is thought to thin and pinch-out to the S and SW, (Figure 3; Gatliff et al., 1994; Stewart and Clark, 1999), but this is based upon limited well control and is only poorly constrained spatially. This is a major uncertainty in the calculation of the storage capacity of the area (section 4.4). Three models are considered for the nature of the Rotliegend pinch-out: faulted, sedimentary and erosive (Fig. 7). The nature of the pinch-out has implications for the rock properties close to the margin, which are unknown due to a lack of borehole penetrations. As the Northern Permian Basin has an approximately concentric arrangement of facies (Gatliff et al. 1994) it is possible that the study area has a facies change compared to the cored areas which are 10's of km to the East. Marginal facies are likely to be alluvial sands and gravels from rivers fed from the Mid-North Sea High to the

south of the study area. In some locations such gravels form the base of the formation as a conglomerate with quartz, quartzite and basalt clasts (30/16-8; Gatliff et al. 1994). According to Heward (1991) this conglomerate in-fills low points in the sub-Permian topography. A conglomerate facies is cored in borehole 29/25-1. Borehole 28/12-1 has a thin sequence of Rotliegend (20 m) suggesting that it is relatively close to the pinch-out, but there is no core available. If the edge of the Rotliegend is controlled by erosion or faulting (Fig. 7), then it is likely there that is no change in sedimentary facies. While the storage capacity would not be significantly altered by the precise geometry of the pinch-out, if the porous aeolian sediments were replaced by a less porous facies then the capacity might be reduced. Given the significant uncertainty in the location of the pinch-out, then the effect of a facies change is only a secondary source of uncertainty.

Although the Rotliegend reservoir has been modelled here as uniform, in detail there are four facies associations that can be distinguished (Heward et al., 2003). Of these, the Weissliegend is the informal name given to the top of the Rotliegend (Fig. 2), with variable thickness from 0 – c. 20 m in UK Quadrant 30 (Heward et al., 2003). As the name implies, it is generally a white or grey colour, in contrast with the brick red underlying Rotliegend. The sands are described as water lain, though some may be slumped or partly remobilised aeolian sands that occurred as the climate became wetter, prior to the flooding of the area by the waters that deposited the overlying Marl Slate (Kupferschiefer). In general, the Weissliegend has poorer reservoir properties than the underlying sands, though the Auk Field is exceptional in that these sands have the highest permeabilities (e.g. Heward et al., 2003; Stromback & Howell, 2002).

The thickness of the Weissliegend is notoriously difficult to map, though Stromback & Howell (2002) claimed to be able to relate the thickness to the pre-Zechstein topography for the Southern North Sea Basin. This sort of detailed mapping is clearly impossible for the study area given the current level of knowledge, however the general conclusion that the Weissliegend is thicker in interdune areas might be of predictive value (Stromback & Howell, 2002, their Fig. 12).

In addition to facies variation within the reservoir, there may be structurally-imposed heterogeneities. Faulting and deformation in clean aeolian sandstones such as the Rotliegend usually occurs by the formation of deformation bands as seen in Rotliegend-equivalent sands exposed onshore in the UK (Edwards et al., 1993; Fig. 5). Each deformation band has a movement of only a few millimetres, so that a large fault can comprise many hundreds or thousands of individual bands. Permeability across the deformation bands is low (Fisher and Knipe, 1998), so they form effective barriers to horizontal fluid flow on the time scale of CO₂ injection. However, there is no evidence of major faulting during the deposition of the Rotliegend (Gatliff et al., 1994) and no evidence of major tectonic events afterwards, at least away from areas affected by halite tectonics which in any case affects the sediments above the Rotliegend. Cores in boreholes 29/25-1 and 28/12-1 have a notable lack of fractures or deformation bands for much of the core, but there are both open fractures (associated with bleaching) and deformation bands towards the base of the cored section in well 29/25-1. From this it is concluded that it is unlikely that there will be large scale barriers to fluid flow within the

Rotliegend reservoir, and that reservoir compartmentalisation is not likely to have occurred. It should be noted that this is in contrast with the intensely compartmentalised Rotliegend gas reservoirs of the approximately coeval Leman sandstone in the southern North Sea (e.g. McCrone et al., 2003).

There is only minimal reservoir quality data from the study area: the composite log (released by the UK Government) in borehole 29/25-1 gives Rotliegend porosity as approximately 20 % (depth interval 8770 – 9400 ft driller’s depth) and approximately 15% (at 9400 – 10038 ft driller’s depth). Reservoir data from the Auk, Argyll and Innes fields that lie within 50 km of the eastern edge of the study area (Fig. 3) are also available as analogues or proxies (Heward et al., 2003). The most likely mean values for porosity and horizontal permeability of the Rotliegend Sandstone reservoir were taken to be 15 % and 100 mD respectively (Table 1). Although these are informed by the available data, they are subject to a degree of uncertainty that is a source of risk to the proposed storage plan. Either a lower than expected permeability could limit the rate of safe injection into the formation (Heinemann et al., 2011) or a lower than expected porosity could reduce the storage capacity. The latter problem would only occur if the regional porosity were lower than expected, and is perhaps unlikely unless the porosity data from analogue hydrocarbon fields is not representative of data from the associated aquifer. It has been suggested that hydrocarbon charging prevents cementation within a reservoir, so that hydrocarbon filled zones may have significantly better reservoir properties than contiguous water filled zones. The relationship between porosity preservation and

hydrocarbon charging has proved to be controversial (e.g. Wilkinson and Haszeldine, 2011) and is still unresolved.

The injectivity of the injection site is a more difficult problem, in that it requires the accurate prediction of the properties of a relatively small volume of rock in the immediate vicinity of the borehole, although the regional permeability will clearly also influence injection and the long-term fate of the CO₂. The difficulty of the prediction will depend upon the nature of the sedimentary system that formed the reservoir – some systems are more homogeneous (and predictable) than others. In this case, the aeolian system is relatively homogeneous compared to other sedimentary facies in that there are unlikely to be significant volumes of non-reservoir sediment within the sequence. In contrast, in a fluvial or other channelised system, at sufficient depths to prevent the imaging of the channels by seismic surveying, the choice of the exact drill site may be very difficult.

There are several strategies that might reduce uncertainty ahead of drilling. Poro-perm conventional core analysis could be obtained from the cores, to enable calibration of remote sensing. Newer seismic reflection surveys at 3D spacing, or with improved bandwidth could provide much better resolution of the reservoir top-surface topography, and internal structure – including porosity estimation via attributes. A sedimentological study of the area in terms of modern or ancient analogues, or a diagenetic study of analogue areas of the reservoir, with special attention to any effects of hydrocarbon charging, might further increase confidence in likely porosity distribution. Ultimately, drilling a test borehole into the reservoir at the proposed injection site, and undertaking

pilot-scale injection of CO₂ is the best way to reduce the uncertainty of these key parameters.

4.2. Seal

The Rotliegend sediments are overlain by carbonates and evaporites of the Upper Permian Zechstein Group, a complex series deposited as a series of wetting and drying cycles during the Late Permian (Gatliff et al., 1994). There is significant lateral variation in facies. To the east (most of Quadrant 29) the Zechstein is mostly halite with only thin interbedded carbonates and anhydrite. To the west, there are areas within Quadrant 28 that entirely lack halite. Most of Quadrant 28 is intermediate in lithology, with interbedded halite and dolomite / anhydrite (Gatliff et al., 1994; Stewart and Clark, 1999). Where significant halite is present, this forms an ideal seal – effectively no porosity or permeability and self-sealing if fractured by tectonic activity. The distribution of halite is a product of three factors: the original depositional thickness; post-depositional thinning due to dissolution in groundwater; and post-depositional thinning and thickening due to the plastic deformation (flow) of the halite, termed halokinesis.

According to Stewart and Clark (1999), thick halite was originally deposited over the entire area, except for the SW-most corner of Quad 28 (Fig. 3). Stewart and Clark (1999) map the distribution of the halite using seismic facies analysis, and they recognise 4 facies types of which 3 contain halite. In Figure 3 the limit of the halite is drawn at the centre of their seismic facies 2, which is shown as the facies in which the halite thins

significantly. Glennie et al. (2003) shows a more limited distribution of halite (Fig. 3). The original thickness for the entire Zechstein was 300 –1200 m (Stewart and Clark their Fig. 2) though halokinesis has largely obscured the original patterns of thickness variation (Gatliff et al., 1994).

Halite movement can result in ‘grounding’ i.e. where the halite thins to zero thickness and the stratigraphy above and below the halite come into physical contact. The same effect can be produced by dissolution during exposure to circulating groundwater. In either scenario the halite ceases to be an effective seal. As an example, in borehole 29/8b-1 (Fig. 3) there is only a thin (10m) dolomite limestone separating the Rotliegend from the overlying Triassic Bunter Shale (from the composite borehole log released by the UK Government). The geographical extent of halokinesis is mapped by the pattern of thickness variations in the overlying Triassic sediments, where halite was dissolved or flowing away from an area, then sedimentation occurred Stewart and Clark (1999; Fig. 3). This led to the development of so-called mini-basins or pods which are visible on regional seismic.

Where the Zechstein thins to c. 150 m, as it onlaps onto the mid-North Sea High to the south of Quad 30, the sequence is dominated by dolomitic carbonates and anhydrite. Typically the anhydrite forms c. 10 - 50% of the total sequence, so an effective seal may be present even if the sequence is only 150 m thick. The nearby hydrocarbon fields of Auk, Argyll and Ardmore (Fig. 3) have non-halite Zechstein seals (Trewin et al., 2003) which proves the seal effectiveness for hydrocarbons, and by inference for CO₂.

4.3. The proposed storage site

The Rotliegend Formation pinches out against the mid-North Sea High to the south and west of the study area (Fig 3). We here propose that CO₂ can be injected to the NE of the pinch-out (Fig. 3), so that the CO₂ will migrate up-dip towards the pinch-out in a south-westerly direction. During migration, some CO₂ will become trapped by residual saturation trapping along the migration path, or by dissolution into the pore water (Ghanbari et al., 2006). If there are adequate seals at the pinchout, the remaining CO₂ will accumulate here. If not, some of the CO₂ will migrate into either the vertical or lateral seal. Quantifying the CO₂ retained by residual saturation, and assessing the likelihood of any remaining CO₂ being retained at the pinch-out are two of the important factors in understanding the performance of the site for CO₂ storage.

The proportion of the migrating CO₂ plume that would be trapped by residual saturation would depend upon, amongst other factors, the distance between the injection site(s) and the pinch-out. The further the migration distance then the greater proportion of CO₂ would be expected to be trapped during migration, and the less would remain to be trapped at the pinch-out. Hence, a valid question becomes: how far to the NNE can the CO₂ be injected? There are two aspects to this question, determined firstly by the lateral extent and security of the seal, and secondly by economics. As the Rotliegend Sandstone dips to the NNE away from the Mid-North Sea High, the further away from the pinch-out a borehole is located the deeper it will be. Deep boreholes are usually more expensive

than shallow ones, so that injecting the CO₂ further way from the pinch-out, to increase residual saturation trapping, will be more expensive. The increased depth does not lead to increased CO₂ density, in fact the calculated density very slowly decreases with increasing depth (Fig. 8) so that there is no advantage to be gained in terms of overall storage capacity. The cost implications are not further considered here. Below, we assume injection will occur at a distance of between 10 and 40 km to the NNE of the pinch-out of the reservoir.

There is only a single borehole in this area, 29/27-1. This is an advantage for the area as a possible storage site, as leakage from abandoned boreholes is a major issue when considering more conventional CO₂ storage in depleted oil and gas fields. The converse is naturally that there is little control on the location of key features. If future boreholes are drilled, careful consideration must be given to possible detrimental effects on the natural geological seal in this region.

4.4. Storage capacity estimate: pore pressure, temperature and porespace

A simple calculation was used to estimate the volume of CO₂ that can be stored in the proposed storage area. If pressure increase is the limiting factor in the CO₂ storage capacity, then there are two locations where rock is most likely to fracture. The first is at the injection site, where pressure increases relative to background are the highest, the second is at the most shallow point in the reservoir where a column of relatively low density CO₂ can produce large differential pressures acting upon the seal. As the injection

site is unknown at this stage, and pressures there can to some extent be controlled by the design of the injection facilities, we will consider the case of pressure increase at the highest point of the reservoir. The depth of this point is not known exactly, but from Fig 3 is close to 2000m. To calculate the permissible pressure increase within the reservoir, both the initial pressure and the maximum permissible porefluid pressure (that will not cause fracturing) must be estimated.

Porefluid pressure data within the area define an approximately linear trend (Fig. 9). These are slightly overpressured relative to a fresh-water hydrostatic gradient and may simply reflect high water densities due to the dissolution of the Zechstein halite. The initial reservoir pressure at 2000m is estimated as 23 MPa. The rock strength is unknown, but can be estimated using fracture pressures presented by Gaarenstroom et al. (1993) for the Central North Sea (Fig. 10). This suggests a fracture pressure of c. 30 MPa. The maximum permissible pressure increase would therefore from 23 to 30 MPa, i.e. 7 MPa. Here we use a pressure increase of 5 MPa to be conservative. To calculate the density of the stored CO₂, the temperature must also be known. Local subsurface temperature data would be useful given the high conductivity of the Zechstein halite, but there are insufficient downhole readings available from within the study area to make reliable corrections for the effects of drilling. Hence, temperatures are estimated from the regional temperature gradient of close to 35°C / km (Kubala et al., 2003), and an assumed sea floor temperature of c. 5°C. The density of CO₂ is estimated to be 709 kg /m³.

The volume of the storage reservoir must also be known. Allowing for the uncertainty in the location of the pinch-out of the Rotliegend (section 4.1), then injection will be at a distance of between 10 and 40 km to the NNE of the pinch-out of the reservoir. The reservoir can be considered to be a triangular prism, with a strike dimension of 50 km, a dip length of 10 – 40 km, and a maximum thickness of 0.5 km. This gives a gross reservoir volume of 125 - 500 km³. However, the Rotliegend reservoir continues to the N and E of the area. While CO₂ is not expected to migrate in this direction due to buoyancy effects, the reservoir can absorb pressure increases. Hence, it is assumed that the volume of reservoir to the NNE of the injection site is equal to the volume to the SSW, a conservative assumption as the Rotliegend generally thickens to the NNE, yielding a gross reservoir volume of 250 – 1000 km³. The reservoir volume must be corrected using the net:gross ratio and the porosity, to produce the pore water volume. Because of the lack of non-reservoir facies within the Rotliegend, a net:gross ratio of 1 can be assumed. Hence we assume a conservative average porosity of 15 % (see section 4.1), giving an estimate of pore water volume of 38 – 150 km³.

The storage volume is estimated using Equation 1 from Chadwick et al. (2008):

$$V_{\text{co2}} = V_{\text{pw}} \cdot (C_r + C_w) \cdot \Delta p \cdot \rho_{\text{CO}_2}$$

where V_{co2} = volume of CO₂ stored, V_{pw} = pore water volume, C_r = pore compressibility of reservoir rock, C_w = water compressibility, Δp = the maximum permissible change in reservoir pressure, and ρ_{CO_2} = the density of CO₂. Numerical values are listed in Table 4.

This yields storage estimates of 170 – 690 Mt CO₂ depending upon the distance between the injection boreholes and the pinch-out of the reservoir. This equates to a storage efficiency of 0.65 %.

This estimate is conservative (i.e. low), and the real figure may be higher. It has been assumed that the boundaries to the Rotliegend will not allow water to flow through them. In reality, any water flow out of the reservoir will reduce pressures within the storage reservoir (Zhou et al., 2008). Other factors that may influence the suitability of the reservoir for CO₂ storage are discussed below. It is important to recall that this is the estimated CO₂ storage capacity of a 50km long section of the Rotliegend margin. Gatliff et al. (1993) show that the margin is approximately 300 km in length between the Devil's Hole Host to the west and the international (UK-Norway) boundary to the east, suggesting that the total storage capacity of the Formation may substantially exceed the above figure. Each section of the Rotliegend margin would require individual assessment for performance during CO₂ storage.

4.5. Permian volcanic rocks

Volcanic rocks within the Rotliegend will have both low matrix porosities and permeabilities, although fracture porosity could be present. As such they represent volumes with minimal effective storage capacity that could be present within the proposed storage area, and these would clearly reduce the storage capacity of the reservoir. A series of thematic papers in Wilson et al. (2004) summarises the distribution

of Permo-Carboniferous volcanism in North West Europe, and the known distribution of Permian volcanic rocks within the Central North Sea is shown in Glennie et al., (2003). They show that Rotliegend volcanic rocks are thickly developed in Poland and Germany, but are known from only a few borehole penetrations in the UK sector of the North Sea (including in core from borehole 29/25-1 examined for this study), where their full extent beyond Quadrants 31 and 39 has yet to be established. Onshore in the UK, contemporaneous extrusive volcanism is sparsely preserved at the base of the Permian succession both in the Midland Valley and south-western parts of Scotland, also in Northern Ireland, where an exploratory geothermal borehole at Larne proved comparable basic volcanic rocks (Penn et al.1983). These isolated outcrops demonstrate that the proven offshore occurrences in the Central North do not mark the western limit of the Permo-Carboniferous volcanic province and suggest that the regional distribution of volcanic rocks is probably controlled by major Carboniferous rift structures. Onshore in Northern England and Southern Scotland, associated intrusive magmatism is widespread in the form of the Whin Sill, the Midland Valley Sill, and their related suite of basic dykes (Smith, 1992; Smythe, 1994).

The sparse provings of Permo-Carboniferous basic volcanic rocks in the UK sector of the Central North Sea were assigned to the Inge Volcanics Formation by Cameron (1993; Fig. 2). Recent studies of these rocks, supported by seismic interpretation, have shown that Inge Volcanics Formation includes at least two separate episodes of volcanism (Martin et al. 2002). The older episode occurs within a predominantly red bed (sandstone and mudstone) succession of late Westphalian age. Resting unconformably on these red

beds, the basal Permian Gensen Formation consists of a thin fine-grained clastic unit, which is overlain by a sequence of younger (Lower Rotliegend) volcanic rocks (Fig. 2). Seismic data from the area of Quadrants 31 and 39 suggest that a second, younger unconformity separates this basal Permian succession from the overlying (Upper) Rotliegend sandstones of the Auk Formation. In one borehole on the Mid North Sea High, Auk equivalent sandstones are absent and Zechstein carbonates and evaporites rest directly upon the Inge Volcanic Formation. Other borehole data show that the Upper Rotliegend interval is also overstepped by basal Zechstein sediments on the Devil's Hole High to the West of the study area. Uncertainty about the age and regional distribution of Permo-Carboniferous unconformities introduces a significant element of doubt into present reconstructions of the early Permian structure and palaeogeography of the Mid North Sea High.

In Quadrant 29, the interpretation of volcanism on the Mid North Sea High is further complicated by the occurrence of rocks related to the Puffin volcanic centre of Mid Jurassic age (Smith and Ritchie, 1993). These form an extrusive succession, which is preserved locally in halite withdrawal structures between block 29/14 and the margin of the West Central Graben. Related intrusions occur within the Zechstein, where they may be confused with volcanic rocks of Permian age (Dixon et al. 1981). The conclusion is that it is uncertain whether Lower Permian age volcanic rocks are present within the proposed study area, and that these present a risk to the drilling of a test borehole and the choice of a storage location. Given the significant uncertainty in the storage capacity estimate, the effect of volcanic rock within the reservoir volume (but spatially removed

from the injection site) is only a secondary risk. Further appraisal work involving seismic surveying might be expected to image volcanic rocks due to their substantial impedance contrast compared to porous sediments, provided that good data can be obtained from below the Zechstein evaporates.

4.6. Chemical interaction between the injected CO₂ and the reservoir rocks.

When large volumes of CO₂ are introduced into a sandstone reservoir, there may be chemical reactions initiated which may dissolve and/or precipitate solid minerals such as calcite or dolomite (Wilkinson et al., 2009). These are of interest for three reasons:

- 1) Mineral dissolution may affect the rock integrity of the target formation or the cap rock (Gundogan, 2011).
- 2) The minerals may form close to the borehole and reduce injectivity (Bacci et al., 2011). Evaporation of porewater into CO₂ can produce a similar effect, by enabling precipitation of salts from saline porewater.
- 3) The minerals may lock-up CO₂ in solid form ('sequester' it) hence preventing the possibility of escape back to the surface (IPCC, 2005).

Computer models of water-rock interaction during CO₂ storage sometimes predict that large volumes of minerals will form (see Wilkinson et al., 2009). We suggest that significant volumes of minerals will not form, as in the UK North Sea there are several oil and gas fields with exceptionally high levels of CO₂ that have been present in the

reservoirs for 10's of millions of years. There are almost no detectable minerals precipitated within these reservoirs from the CO₂ (Wilkinson et al., 2009; Lu et al., 2011). We conclude that it is unlikely that there will be sufficient chemical reaction between the reservoir sandstone and the injected CO₂ to significantly alter the mass of free-phase CO₂ within the reservoir, and so this is neglected in the preliminary modelling. However, relatively minor dissolution of the reservoir rock around an injection borehole could potentially generate fines leading to a loss in injectivity. Given the lack of experience in CO₂ injection into a Rotliegend reservoir, it is difficult to quantify this risk.

4.7. Lateral Seal – Devonian and Carboniferous

If the CO₂ migrates to the pinch-out of the Rotliegend as shown by the modelling, then it will encounter the underlying formations (which are structurally higher to the SW of the pinch-out, Fig 4). These formations will be either sediments of Devonian and/or Carboniferous age, or low permeability Silurian strata that can be regarded as 'basement'. The thickness (or existence) of the Devonian and/or Carboniferous sediments is one of the major uncertainties of the proposed storage area.

The Carboniferous sediments are not present everywhere in the study area, they die out on the Mid-North Sea High with a SW limit probably not much different to the Rotliegend (Gatliff et al., 1994). It is shown as absent from the proposed storage area both in Maynard et al. (1997) and Martin et al. (2002), though these are demonstrably incorrect, as neither of these papers show the established Carboniferous basin below the

northern half of Quad 29. The Carboniferous is absent in borehole 28/12-1 which penetrates into probable Devonian which has been cored. The Carboniferous in this area is expected to be shallow marine and fluvio-deltaic in origin (Gatliff et al., 1994), i.e. to consist of potentially permeable sandstones interbedded with low permeability mudstones. The degree of connectivity of the sandstones will control to what extent they form potential leakage pathways, and this is difficult to assess.

Where Devonian sediments directly underlie the Rotliegend, then in the absence of cores from boreholes or age-diagnostic fossils, the sediments are often only separated from the Lower Permian by electric log response – the Permian is more homogeneous (Gatliff et al., 1994). Where the Devonian is overlain by Carboniferous sediments it is equally difficult to separate. Gatliff et al. (1994), in a regional description of the Devonian, show that the sediments thin or disappear over the Mid-North Sea High, but also state that the Upper Devonian is present everywhere in the area. The sediments are medium to fine-grained sand-dominated non-marine units that includes thin limestones, shales and anhydrite that are laterally variable (Gatliff et al., their Fig. 14). There is no porosity or permeability data from Devonian strata close to potential storage site. Core within borehole 29/25-1 that is identified as Devonian on the borehole logs contains vertical structures that we interpret as roots, suggesting (but not proving) a Carboniferous age. Borehole 28/12-1 has Devonian core, brick red fluvial fine grained sands and silts with occasional rip-up clasts.

Analogue data are available from the Stirling Field, which lies some 150 km to the north of the study area, with an average matrix permeability of 0.68mD and an average porosity of 9.5% at c. 3000 m depth (Gambaro and Currie, 2003). The Devonian strata are heterogeneous due to both the nature of the sedimentary facies (braided fluvial deposits with interbedded overbank sediments; Gambaro and Currie, 2003) and due to post-depositional fracturing. As an alternative analogue, the Buchan Field (in the Witch Ground Graben some 100 km north of the study area) has a fractured Devonian reservoir with low matrix permeability (Benzagouta et al., 2001). Fracture intensity correlates with lithology, e.g. clean, well sorted sands are highly fractured. Given the sand-dominated nature of the Upper Devonian sediments, there must be at least the possibility that they could form an ineffective lateral seal to the proposed stratigraphic trap. There is then a theoretical risk of the stored CO₂ migrating thorough laterally continuous pre-Zechstein strata either to outcrops on the UK mainland or on the seabed. In either case, the distances for migration would be long; being 180 km minimum. Retention of CO₂ by small topographic traps beneath the upper surface of the migration route, and residual saturation and dissolution makes it improbable that leakage to seabed would occur; although that has not been modelled.

4.8. Seismicity

As natural earthquakes could potentially disrupt a storage seal, a brief study of the seismicity of the potential study area was conducted by examining the British Geological Survey earthquake database (Fig. 11). The completeness of the earthquake catalogue

varies with time. In the Central North Sea, for earthquakes with a magnitude of 3 ML (local magnitude), it is only certain that all events appear in the catalogue for the period covered by modern instrumental monitoring (post-1970). It is unlikely that magnitude 4 ML or smaller earthquakes in this area would have been reported prior to instrumental monitoring due their distance offshore. Even for larger events, early instrumental records would be required to determine the location and size of an earthquake. However, since about 1700, it is likely any North Sea earthquakes of magnitude 6 ML or greater (that is, those which can be felt in all the surrounding countries) would have been reported and located.

The general area is one of relatively low seismicity, which lies to the west of a region of slightly higher seismicity associated with the Central Graben. The Central Graben is itself significantly less active than the Viking Graben to the north. Earthquakes tend to be small and shallow, and seismicity is not concentrated on any single fault but rather indicates activity spread over a series of faults. Bungum et al. (1991) report that epicentre uncertainties for events in this area are of the order of 15 km horizontally.

There is one recorded earthquake within Quadrants 28 and 29; the 26 April 1978 (3.1 ML) event (Fig. 11). Two other events lie close to the north-eastern corner of the area (4 June 2007, 3.9 ML; and 24 July 2007, 3.1 ML). Both of these earthquakes were shallow (5 km or less) and no focal mechanisms are available. The largest event in this region, the 7 May 2001 Ekofisk event, lies approximately 140 km east of the area (Ottemöller et al., 2005). This had a local magnitude of 4.2 and a depth of less than 3 km indicating that the event occurred in the overburden. Seismological analysis indicates that the event was

induced by stress changes caused by unintentional water injection into the overburden. Slip probably occurred on a near-horizontal plane. Ottemöller et al. (2005) point out that the combined effect of the low stress drop and low overburden shear strength was that the event released less high frequency energy than a typical stress drop event with similar source dimensions. The event was felt strongly on platforms and associated structures in the Ekofisk oil field but did not cause damage (Ottemöller et al., 2005). There are also several non-induced smaller events (around 2.5 – 3.5 ML) in this area in the catalogue.

Within 150 km to the north of Quadrants 28 and 29, there are four earthquakes ranging from 2.3 to 3.2 ML. These are widely dispersed and are not associated with a single structure. There are no earthquakes in the database between the study area and the UK mainland. In conclusion, there is no good historical reason to expect earthquakes in the region of the potential storage site. In conclusion, seismicity is a very low risk in the performance of the storage site.

4.9. Neotectonics

Although the Quadrant 28-29 area is one of low recorded seismicity, seismic reflection data from the area show that Cenozoic faults, often with a substantial displacement, are widely developed. Stratigraphic evidence shows that these faults were most active during the Eocene (c. 40 Ma ago; Fig. 12). They probably formed when uplift of the UK, combined with continued subsidence in the North Sea, increased the eastward dip of the West Central Shelf. This tilting was sufficient to generate a series of low angle

detachments within the post Zechstein succession of the shelf. These detachments produced NNW-trending en echelon faults at top Cretaceous level, which are parallel to the main axis of Cenozoic subsidence in the Central North Sea. Extensional fault movement on the shelf may be compensated by contemporaneous contractional deformation within the Central Graben itself. Many of the faults extend almost to the seabed (Fig. 12). The largest of the faults are associated with hanging wall roll-over anticlines that have provided a speculative target for hydrocarbon exploration. The faults may provide a migration pathway through the Chalk Group for fluids from deeper in the basin, even without the development of halite grounding. This would be a local pathway for fluids that had already breached the Zechstein seal. Such breaching is only a significant risk in areas with halite diapirism and dissolution (Fig. 3). These faults could adversely affect local CO₂ storage in Cretaceous sands but are not relevant to storage in the deeper Rotliegend sandstones below the Zechstein halite seal.

4.10. Limitations of the study

This evaluation has been undertaken using published information. Because of the limited data available, significant uncertainties remain in the following issues:

- 1) The location of the margin (pinch-out) of the Rotliegend reservoir to the SW. This affects the volume of storage reservoir, the length of migration path before the CO₂ reaches this point, and the nature of the overlying seal, i.e. the reservoir may extend beyond the minimum likely extent of the halite. Analysis of seismic survey

data might improve confidence, though imaging below the halite in the Zechstein is difficult.

- 2) The location of the facies change within the Zechstein, from halite in the N and E, to dolomite and anhydrite in the SW. As halite is the ideal seal, while the performance of the dolomite and anhydrite is uncertain, this has important implications for the top seal efficiency, although modelling of CO₂ migration showed that the dolomite / anhydrite seal did retain CO₂. Again, seismic survey analysis might improve certainty.
- 3) The coverage of the Mid-North Sea High by Devonian and Carboniferous sediments is uncertain. This has important implications for the lateral seal. Modelling of the CO₂ in the subsurface could determine the sensitivity of the security to this parameter.
- 4) Generic or analogue data have been used for some key parameters, particularly in the calculation of the CO₂ storage volume. Porosity and permeability, rock fracture strength, and reservoir temperature should ideally all be measured from within the storage area. These parameters determine both storage volume, and injectivity which are key factors in the viability of the storage site.

5. Conclusions

The initial assessment of a saline aquifer may involve a small quantity of data, spread thinly over a large geographical area, as in the case study described here. At the initial stages of appraisal, geological uncertainties should be identified, so that the remainder of the appraisal process is focussed on reducing these uncertainties and consequently reducing the risk associated with any subsequent investment. Any difficult geological questions should be identified, even if there is no possibility of conclusively answering the questions with the data available at this early stage of the appraisal process. This will reduce the risk of an unexpected 'show-stopper' being identified after more investment has been made in the appraisal process. Some of the risk issues may be adequately dealt with at the initial assessment stage, for example in this case the natural seismic hazard is assessed as low risk, and it is unlikely that any further work would be required on this subject even if the project were to reach the stage of actual CO₂ injection.

However it is likely, with limited borehole penetrations in a proposed area, that key geological uncertainties will remain. In this case, the key uncertainties are the extent of the reservoir, the location of the seal transition from halite to dolomite / anhydrite, and the injectivity of the reservoir. It may not be possible to obtain definitive answers to these questions, however the appraisal need not necessarily provide definitive answers, merely produce reasonable evidence that the storage site is adequate for the purpose for which it is intended. For example, the location of the Rotliegend pinch-out is a crucial uncertainty in calculating the storage capacity of the site, but need not be resolved provided that the minimum probable value of the estimated range of capacities exceeds whatever minimum

value the project requires for economic viability. Any capacity above this minimum, which might eventually be proved by CO₂ injection, would effectively be a bonus.

Some geological questions can, given the data available, only be addressed using analogues. For many saline aquifers, data will be derived from neighbouring hydrocarbon fields where, for example, reservoir quality has been measured. As the analogue sites may lie many 10's of kilometres away from the proposed storage site, this introduces a degree of uncertainty that may only be finally reduced by drilling a borehole into the proposed injection site. The injectivity of the reservoir is a key parameter in the economics of an injection project, but given the degree of geological knowledge typical of saline aquifers, will not be fully resolved prior to drilling. An initial appraisal, such as presented here, can give an indication of the heterogeneity of the sedimentary system into which the CO₂ will be injected, and some indication of the range of likely reservoir properties. In this case, the aeolian system is relatively homogeneous in the sense that there are unlikely to be significant volumes of non-reservoir sediment within the sequence, though there is some reservoir quality variation between facies associations.

As a consequence of the evaluations reported in this publication, the proposed CO₂ storage site was deemed to be sufficiently promising for further study, and commercial investment was made to acquire further data in an attempt to reduce key uncertainties.

Acknowledgements

This research was funded by Coots Energy / Progressive Energy, and arranged by John Aldersley-Williams of Redfield Energy. We are grateful for their permission to publish this paper. The British Geological Survey (BGS) provided access to core and samples. KS and SS publish with the permission of the Director of BGS.

References

Bacci, G., Korre, A., Durucan, S., 2011. An experimental and numerical investigation into the impact of dissolution/precipitation mechanisms on CO₂ injectivity in the wellbore and far field regions. *International Journal of Greenhouse Gas Control* 5, 579–588.

Baldwin, B., Butler, C.O., 1985. Compaction curves. *Bulletin of American Association of Petroleum Geologists* 69, 622-626.

Benzagouta, M. S., Turner, B. R., Nezzal F., A. Kaabi, 2001. Reservoir Heterogeneities, in Fractured Fluvial Reservoirs of the Buchan Oilfield (Central North Sea). *Oil & Gas Science and Technology – Revue d’Institute Francaise Petrol* 56, 327-338.

Bungum, H., Alsaker, A., Kvamme, L. B., Hansen, R. A., 1991. Seismicity and seismotectonics of Norway and nearby continental shelf areas. *Journal of Geophysical Research* 96, 2249-2265.

Cameron, T. D.J., 1993. Lithostratigraphic nomenclature of the UK North Sea. Volume 4. Triassic, Permian and pre-Permian (Central and Northern North Sea). British Geological Survey, Keyworth.

Carneiro, J.F., Boavida, D., Silva, R., 2011. First assessment of sources and sinks for carbon capture and geological storage in Portugal. *International Journal of Greenhouse Gas Control* 5, 538-548.

Chadwick, A., Arts, R., Bernstone, C., May, F., Thibeau, S., Zweigel, P., 2008. Best practice for the storage of CO₂ in saline aquifers. British Geological Survey occasional publication 14.

Dixon, J. E., Fitton, J. G., Frost R. T. C., 1981. The Tectonic significance of Post-Carboniferous igneous activity in the North Sea basin, in: Illing, L.V., Hobson, G.V. (Eds.), *Petroleum Geology of the Continental Shelf of North-western Europe*. Institute of Petroleum, London, pp. 121-137.

Duan, Z.H., Moller, N., Weare, J.H., 1992. An equation of state (EOS) for CH₄-CO₂-H₂O I: pure systems from 0 to 1000 C and from 0 to 8000 bar. *Geochimica et Cosmochimica Acta* 56, 2605-2617.

Edwards, H.E., Becker, A.D., Howell, J.A., 1993. Compartmentalization of an aeolian sandstone by structural heterogeneities: Permo-Triassic Hopeman Sandstone, Moray Firth. Geological Society, London, Special Publications 73, 339-365

Fine, R.A., Milero, F.J., 1973. Compressibility of water as a function of temperature and pressure. Journal of Chemical Physics 59, 5529 – 5536.

Fisher, Q. J., Knipe, R. J. 1998. Fault sealing processes in siliciclastic sediments, in: Jones, G., Fisher, Q. J., Knipe, R. J. (Eds.), Faulting, Fault Sealing and Fluid Flow in Hydrocarbon Reservoirs. Geological Society, London, Special Publications, pp. 147, 117-134.

Frykman, P., 2001. Spatial variability in petrophysical properties in Upper Maastrichtian chalk outcrops at Stevns Klint, Denmark. Marine and Petroleum Geology 18, 1041-1062.

Gambaro, M., Currie, M., 2003. The Balmoral, Glamis and Stirling Fields, Block 16/21, UK Central North Sea, in: Gluyas, J.G., Hitchens, H.M. (Eds.), United Kingdom Oil and Gas Fields, Commemorative Millennium Volume. Geological Society, London, Memoir 20, 395-413.

Gaarenstroom, L., Tromp, R.A.J., de Jong, M.C., Brandenburg, A.M., 1993.

Overpressures in the Central North Sea: implications for trap integrity and drilling safety,

in: Parker, J. R. (Ed.), Petroleum Geology of Northwest Europe: Proceedings of the 4th Conference. Geological Society, London, pp. 1308 – 13.

Gatliff R. and 11 others, 1994. Geology of the Central North Sea. UK Offshore Regional Report, BGS, HMSO London.

Ghanbari, S., Al Zaabi, Y., Pickup, G.E., Mackay, E.J., Gozalpour, F., Todd, A.C., 2006. Simulation of CO₂ Storage in Saline Aquifers. Transactions of the Institute of Chemical Engineers 84, 764-775.

Glennie, K.W., Higham, J., Stemmerik, L., 2003. Permian, in: Evans, D., Graham, C., (Eds.), The Millennium Atlas: petroleum geology of the central and northern North Sea. Geological Society, London, pp. 91-103.

Gundogan, O., Mackay, E.J., Todd, A.C., 2011. Comparison of numerical codes for geochemical modeling of CO₂ storage in target sandstone reservoirs. Chemical Engineering Research and Design 89, 1805-1816.

Hatzignatiou D. G., Riis F., Berenblyum R., Berenblyum, R., Hladik, V., Lojka, R., Francu, J., 2011. Screening and evaluation of a saline aquifer for CO₂ storage: Central Bohemian Basin, Czech Republic. International Journal of Greenhouse Gas Control 5, 1429-1442.

Heinemann, N., Wilkinson, M., Pickup, G.E., Haszeldine, R.S., N.A. Cutler, 2011. CO₂ storage in the offshore UK Bunter Sandstone Formation. *International Journal of Greenhouse Gas Control* 6, 210–219.

Heward, A.P., 1991. Inside Auk – the anatomy of an aeolian oil reservoir, in: Miall, A.D., Tyler, N. (Eds.), *The three dimensional facies architecture of terrigenous clastic sediments and its implications for hydrocarbon discovery and recovery. SEPM Concepts in Sedimentology and Paleontology* 3, pp. 44 – 56.

Heward, A.P., Schofield P., Gluyas J.G. , 2003. The Rotliegend reservoir in Block 30/24, UK Central North Sea: including the Argyll (renamed Ardmore) and Innes fields. *Petroleum Geoscience* 9, 295-307.

IPCC, 2005. Special Report, Carbon Dioxide Capture and Storage. Intergovernmental Panel on Climate Change.

Kubala, M., Bastow, M., Thompson, S., Scotchman, I., Oygard, K., 2003. Geothermal regime, petroleum generation and migration, in: Evans, D., Graham, G., Armour, A., Bathurst, P. (Eds.), *The Millennium Atlas: Petroleum Geology of the Central and Northern North Sea*. Geological Society of London, pp. 289-315.

Lu, J., Wilkinson, M., Haszeldine, R.S., Boyce, A.J., 2011. Carbonate cements in Miller field of the UK North Sea: a natural analog for mineral trapping in CO₂ geological storage. *Environmental Earth Sciences* 62, 507-517.

Mallon, A.J., Swarbrick, R.E., 2002. A compaction trend for non-reservoir North Sea Chalk. *Marine and Petroleum Geology* 19, 527-539.

Martin, C. A. L., Stewart, S. A., Doubleday, P. A. 2002. Upper Carboniferous and Lower Permian tectonostratigraphy on the southern margin of the Central North Sea. *Journal of the Geological Society, London* 159, 731-749.

Maynard, J.R., Hofmann, W., Dunay, R.E., Bentham, P.N., Dean, K.P., Watson, I., 1997, The Carboniferous of western Europe: the development of a petroleum system. *Petroleum Geoscience* 3, 97-115.

McCrone, C.W., Gainski, M., Lumsden, P.J., 2003. The Indefatigable Field, Blocks 49/18, 49/19, 49/23, 49/24, UK North Sea, in: Gluyas, J.G., Hichens, H.M., (Eds.), *United Kingdom Oil and Gas Fields, Commemorative Millennium Volume*. Geological Society, London, *Memoir*, 20, 741 – 747.

Moss, B., Barson, D., Rakhit, K., Dennis, H., Swarbrick, R., 2003. Formation pore pressures and formation waters, in: D. Evans, , C. Graham, A. Armour, C. Grahman, P.

Bathurst, The Millennium Atlas: Petroleum Geology of the Central and Northern North Sea. Geological Society, pp. 317-329.

Ogawa, T., Nakanishi, S., Shidahara, T., Okumura, T., Hayashi, E., 2011. Saline-aquifer CO₂ sequestration in Japan-methodology of storage capacity assessment. International Journal Of Greenhouse Gas Control 5, 318-326.

Ottmoller, L., Neilsen, H. H., Atakan, K., Braunmiller, J., Havskov, J., 2005. The 7 May 2001 induced seismic event in the Ekofisk oil field, North Sea, Journal of Geophysical Research 110, B10301.

Penn, I. E., Holliday, D. W., Kirby, G. A., Kubala, M., Sobey, R. A., Mitchell, W. I., Harrison, R. K., Beckinsale, R. D., 1983. The Larne No. 2 Borehole: discovery of a new Permian volcanic centre. Scottish Journal of Geology 19, 333-346.

Smith, K., 1992. Carboniferous magmatism in the Iapetus convergence zone: evidence from deep seismic reflection profiles. Journal of the Geological Society, London 149, 907-914.

Smith, K. and Ritchie, J. D., 1993. Jurassic volcanic centres in the Central North Sea, in: Parker, J. R. (Ed.) Petroleum Geology of Northwest Europe; Proceedings of the 4th Conference. Geological Society, London, pp. 519-532.

Smith, M., Campbell, D, Mackay, E., Polson, D., 2011. CO₂ Aquifer Storage Site Evaluation and Monitoring. Heriot-Watt University, Edinburgh.

Smythe, D. K., 1994. Geophysical evidence for ultra-wide dykes of the late Carboniferous quartz-dolerite swarm of northern Britain. *Geophysical Journal International* 119, 20-30.

Stewart, S.A., Clark, J.A., 1999. Impact of salt structures of the Central North Sea hydrocarbon fairways, in: Fleet, A.J., Boldy, S.A.R., (Eds.) *Petroleum Geology of Northwest Europe*, Proceedings of the 5th Conference. Geological Society, London, pp. 179-200.

Stoker, M.S., Johnson, H., 1986. 1:250000 Series Solid Geology Map, Devil's Hole. British Geological Survey, Keyworth.

Stromback, A.C., Howell, J.A., 2002. Predicting distribution of remobilized aeolian facies using sub-surface data: the Weissliegend of the UK Southern North Sea. *Petroleum Geoscience* 8, 237-249.

Tiab, D. & Donaldson, E., 2004. *Petrophysics*, Elsevier Gulf.

Trewin, N.H., Fryberger, S.G., Kreutz, H., 2003. The Auk Field, Block 30/16, UK North Sea, in: Gluyas, J.G., Hichens, H.M. (Eds.), *United Kingdom Oil and Gas Fields*,

Commemorative Millennium Volume. Geological Society, London, Memoir 20, pp. 485-496.

Vejbaek, O.V., 2002. Reservoir characterization of the Roar Gas Field, Danish North Sea. *Petroleum Geoscience* 8, 71-87.

Wilkinson, M., Haszeldine, RS, Fallick, AE, Odling, N., Stoker, SJ, Gatliff, RW, 2009, CO₂-Mineral Reaction in a Natural Analogue for CO₂ Storage—Implications for Modeling. *Journal of Sedimentary Research* 79, 486–494.

Wilkinson, M., Haszeldine, R.S., 2011. Oil charge preserves exceptional porosity in deeply buried, overpressured, sandstones: Central North Sea, UK. *Journal of the Geological Society* 168, 1285-1295.

Wilson, M., Neumann, E.-R., Davies, G. R., Timmerman, M. J. Heeremans, M., Larsen, B. T., 2004. Permo-Carboniferous Magmatism and Rifting in Europe. Special Publication, Geological Society, London.

Zhou, Q., Birkholzer, J.T., Tsang, C.-F., Rutqvist, J., 2008. A method for quick assessment of CO₂ storage capacity in closed and semi-closed saline formations. *International Journal of Greenhouse Gas Control* 2, 626–639.

Zhou, D., Zhao, Z.X., Liao, J. and Sun, Z., 2011. A preliminary assessment on CO₂ storage capacity in the Pearl River Mouth Basin offshore Guangdong, China.

International Journal of Greenhouse Gas Control 5, 308-317.

Fig Captions

Fig. 1- Location map in North Sea.

Fig. 2 – Simplified stratigraphy, taken from the well log for well 29/27-1; Heward et al. (2003); and Martin et al. (2002).

Fig. 3 – Map showing wells that penetrate the Rotliegend section, or the underlying strata where the Rotliegend is absent for the study area (Quads 28 and 29) and surrounding area. Depth contours of top Rotliegend from Stoker and Johnson (1986) extended using well data. Southern limit of Rotliegend from Gatliff et al. (1994). Limit of Zechstein halite from (1) Glennie et al. (2003) and (2) Stewart and Clark (1999), see text. Limit of halokinesis from Stewart and Clark (1999). Salt diapirs and hydrocarbon fields from Glennie et al. (2003).

Fig. 4 – The cross-section of the model of CO₂ migration, see Fig. 3 for geographical location.

Fig. 5 – Rotliegend sandstone: red-brown low angle laminated sands showing a sub-vertical deformation band. Well 29/25-1, 2697 m drillers depth.

Fig. 6 – Modelled concentration of CO₂ in porewater (left), and saturation of free-phase CO₂ in porespace at 10,000 years after injection (right).

Fig. 7 –Three scenarios for the geometry of the margin of the Rotliegend. These have implications for the distribution of sedimentary facies around the margins.

Fig. 8 –Calculated density of CO₂ for subsurface pressure and temperature conditions.

Fig. 9 - Mud weights from boreholes used as a measure of porefluid pressure within the Rotliegend.

Fig. 10 – Fracture pressures measured as leak-off tests during the drilling of boreholes (Moss et al., 2003). The porefluid pressure gradient in Rotliegend is at 90% of the mud weights, see text. The difference between the initial pressure of the reservoir and the fracture pressure gives a measure of how much pressure increase can be safely accommodated during CO₂ injection, shown as 8 MPa at 2000m depth.

Fig. 11 - Seismicity map for the North Sea region. The rectangle denotes the study area.

Fig. 12 - Geoseismic section across Quadrant 28, showing part of the system of shallow faults, active during the Eocene, which detach upon the underlying Zechstein interval and probably formed as a result of sliding of the post-Permian cover of the West Central Shelf towards the West Central Graben during early Paleogene subsidence (modified and redrawn from Figure 4.16 of Evans et. al., 2003).

Wilkinson et al.

Table 1 – Rock properties used in STARS model.

Age / Formation	Porosity (%)	Horizontal Permeability (mD)	Source
Paleogene and Neogene	30	1.7	Baldwin and Butler (1985), assumes is shale
Chalk	30	7	Frykman (2001); Mallon and Swarbrick (2002); Vejbaek (2002)
Lower Cretaceous	22	0.26	Baldwin and Butler (1985), assumes is shale
Triassic / Jurassic	25	100	unpublished data compilation
Zechstein carbonates and anhydrite	5	10	Trewin et al. (2003)
Zechstein halite	0	0	generic
Rotliegend	15	100	composite well log; Heward et al. (2003)
Devonian / Carboniferous	9.6	0.68	Gambaro and Currie (2003)
Pre-Carboniferous	0	0	generic

Wilkinson *et al.*

Table 2 – Summary of screening results for CO₂ storage reservoirs and seals

Name of unit	Lithology summary ^a	Average porosity (ϕ) and horizontal permeability (K_H) for Stars model	Depth of top surface ^b	Reservoir and seal potential
Paleogene and Neogene	mixed clastics	No data from study area; Baldwin and Butler (1985): assumes shale, $\phi = 30\%$, $K_H = 7$ mD	outcrops on sea bed	none – too shallow
Upper Cretaceous Chalk	fine-grained limestones, some argillaceous	No data from study area, Frykman (2001); Mallon and Swarbrick (2002); Vejbaek (2002) suggest very low permeability values, $\phi = 30\%$, $K_H = 7$ mD	250 – 4250 m	none – low permability unless fractured, unpredictable
Lower Cretaceous	clay dominated	No data from study area; Baldwin and Butler (1985): assumes shale, $\phi = 22\%$, $K_H = 0.26$ mD	750 – 6250m	seal
Jurassic	thin or absent except in NE	Not modelled	?3000 - 7000	low – distribution too limited
Triassic	clay-dominated except in NE	No data from study area; uses unpublished data compilation: $\phi = 25\%$, $K_H = 100$ mD	NA	low – sand distribution too limited
Permian Zechstein halite	halite	nil porosity and permeability	NA	<i>perfect seal</i>
Permian Zechstein dolomite and anhydrite	potentially vuggy dolomites (Trewin <i>et al.</i> , 2003)	$\phi = 5\%$, $K_H = 10$ mD (dolomite, Trewin <i>et al.</i> , 2003). Anhydrite less porous and permeable.	1750 – c. 10 or 12km	<i>good – proven in Auk, Argyll and Innes fields (Fig. 3)</i>
Permian Marlslate	thin (> 5m) dolomitic limestone	negligible unless fractured; too thin to model	1750 – c. 10 or 12km	none – too thin

Permian Rotliegend Sandstone	Aeolian and fluvial sandstones	$\phi = 15 \%$, $K_H = 100$ mD, see text	See Fig. 3	<i>good reservoir, almost all sandstone, very few interbedded shales</i>
Devonian & Carboniferous	?fluvial / alluvial clastics	$\phi = 9.6 \%$, $K_H = 0.68$ mD, Gambaro and Currie (2003)	NA	none
Pre-Carboniferous	metamorphosed greywackes	assumed negligible	NA	none

^b Source: Gatliff et al., (1994)

^a Source: Stoker & Johnson (1986)

Table 3

Table 3 – The distribution of Rotliegend sediments in the study area and surrounding area from well penetrations

Well (* core)	Depth top Rot / m	Thickness / m	Underlying stratigraphy (* core)
26/7-1	1108	152	Carboniferous*: grey mudstones with subordinate thin coals and limestones, white / grey sandstones up to 50m thick
26/8-1	1441	390 (982?)*	Carboniferous: alternating grey sands and muds, coals below 2730m
26/12-1	absent (928)	0	Devonian - ?Silurian: red-brown sands and muds, 2 – 3m conglomerate on top
26/14-1	1102	8.5	Lower Devonian - ?Silurian: grey - pink sands, red – green muds alternating.
27/3-1	absent (1352)	0	Lower Paleozoic (undifferentiated): red – purple silty sands, sands, conglomerates and shales.
27/10-1	absent (1464)	0	Lower Paleozoic (undifferentiated): no description
28/5-1	2810	126	?Devonian: white to brown sands and shales
28/12-1*	2187	20	?Devonian: red-brown silts and sands, minor conglomerate
29/8b-1*	3722	> 149	not penetrated
29/13b-2	3979	> 63	not penetrated
29/14b-2	4035	> 193	not penetrated
29/18-1	3281	> 525	not penetrated
29/19a-2	2806	> 146	not penetrated
29/19a-3	2717	> 323	not penetrated
29/25-1	2649	433	?Devonian*: red clays and sands
29/27-1*	2789	> 79	not penetrated
30/21-1	2618	> 44	not penetrated
30/23-1*	2688	53	?Devonian: reddish brown sands, apparently only shale at top
30/27-1	2439	> 152	not penetrated
30/28-1	2531	> 298	not penetrated
30/30-1	2907	59	?Devonian: red-grey sands and shales, interbedded
30/30-3Z	2996	> 104	not penetrated
36/13-1	absent (1235)	0	Carboniferous: alternating grey-brown shales and sands
36/15-1	absent (1637)	0	?Devonian: grey – red sands and alternating shales
36/23-1	absent (1747)	0	no description (drilled 1969)
36/26-1	1460	? 5	Carboniferous: grey sands and black shale / coal
37/10-1	absent (1799)	0	Devonian / Carboniferous: alternating red sands and shales

37/23-1	absent (2282)	0	? Devonian / Carboniferous: alternating red sands and shales
37/25-1	absent (2045)	0	Upper Devonian: alternating grey-brown sands and shales
38/1-1	absent (1877)	0	? Devonian / Carboniferous / Permian: alternating sands and shales
38/3-1	2154	59	*Devonian: sands and thin interbedded shales
38/10-1	2378	133***	?Devonian: interbedded sands, shales, conglomerates, defined by increased clay content
38/16-1	absent (1904)	0	Carboniferous: alternating shales and sands with coals
38/18-1	absent (2332)	0	Carboniferous: alternating shales and sands
38/24-1	absent (2431)	0	Undifferentiated: grey / red alternating shales and sands

** 592 m of strata described as Permo-Carboniferous (undifferentiated), base Rotliegend drawn at 75m thick mudstone

*** includes volcanics

TD too shallow: 28/5a-6, 28/10a-2, 29/24-1, 30/28-2, 29/24-1, 29/19-1, 29/14-5

No strat: 37/12-1, 38/22-1 (turbo-drilled through relevant section)

Missing from CDA: 29/14-4 (should penetrate)

Wilkinson et al.

Table 4 Summary of data used for calculation of storage total

Depth	2.65 - 2.86km	see Fig. 3
reservoir thickness	0 - >500m	see Table 3
distance from injection point to pinch-out	10 – 40 km	see text
strike length	50 km	see text
average porosity	15 %	lowest value from composite well logs
pore compressibility of reservoir rock (C_r) well sorted sands at 23 MPa	$8.7 \times 10^{-4} / \text{MPa}$	Tiab & Donaldson (2004)
water compressibility (C_w) at 75°C and 23 MPa	$4.3 \times 10^{-4} / \text{MPa}$	Fine and Milero (1973)
maximum permissible pressure increase	5 MPa	see text
CO ₂ density	709 kg / m ³	Duan et al. (1992)

Figure 1
[Click here to download high resolution image](#)

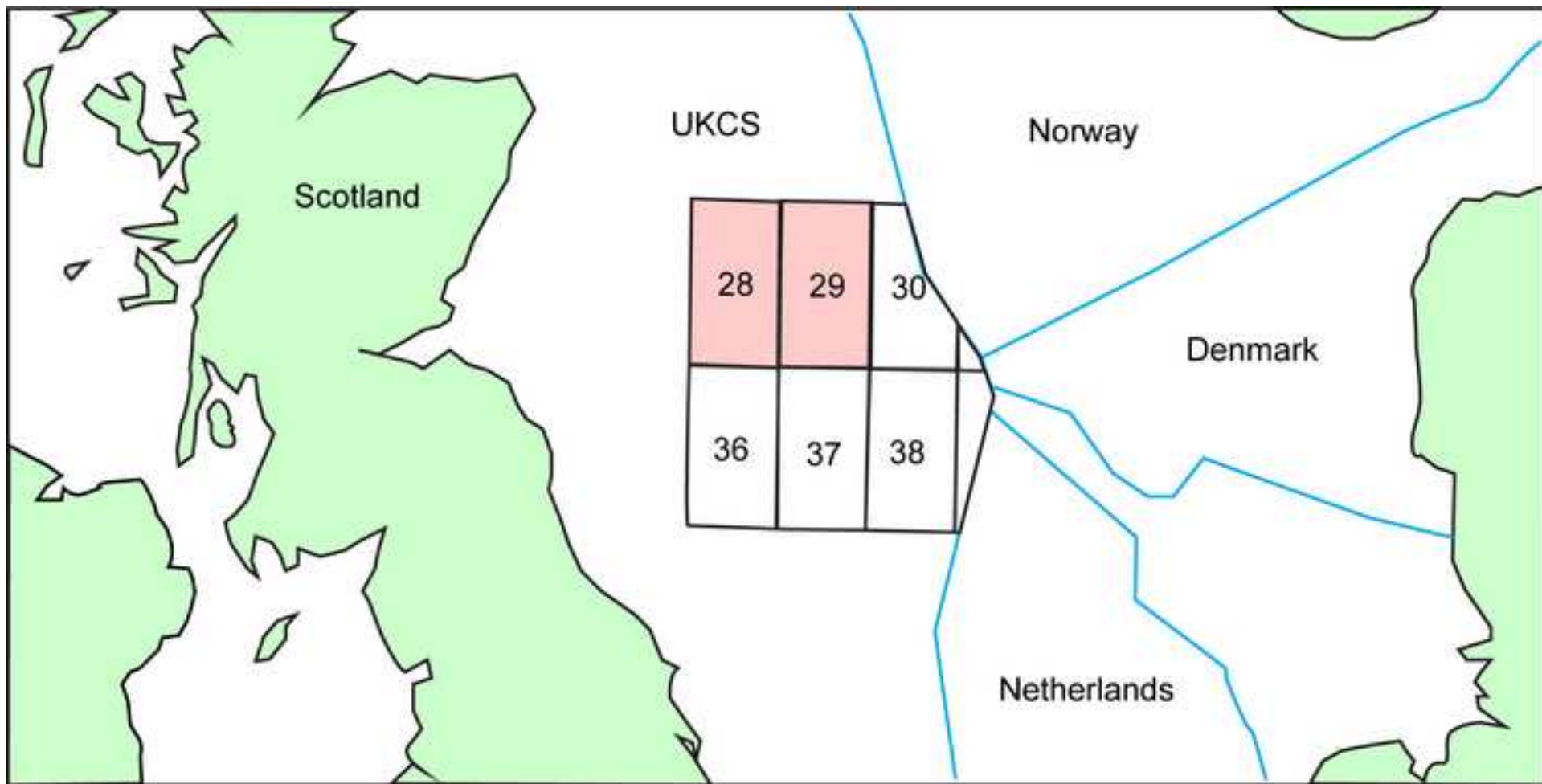


Figure 2
[Click here to download high resolution image](#)

Martin et al. (2002)

Heward et al. (2003)

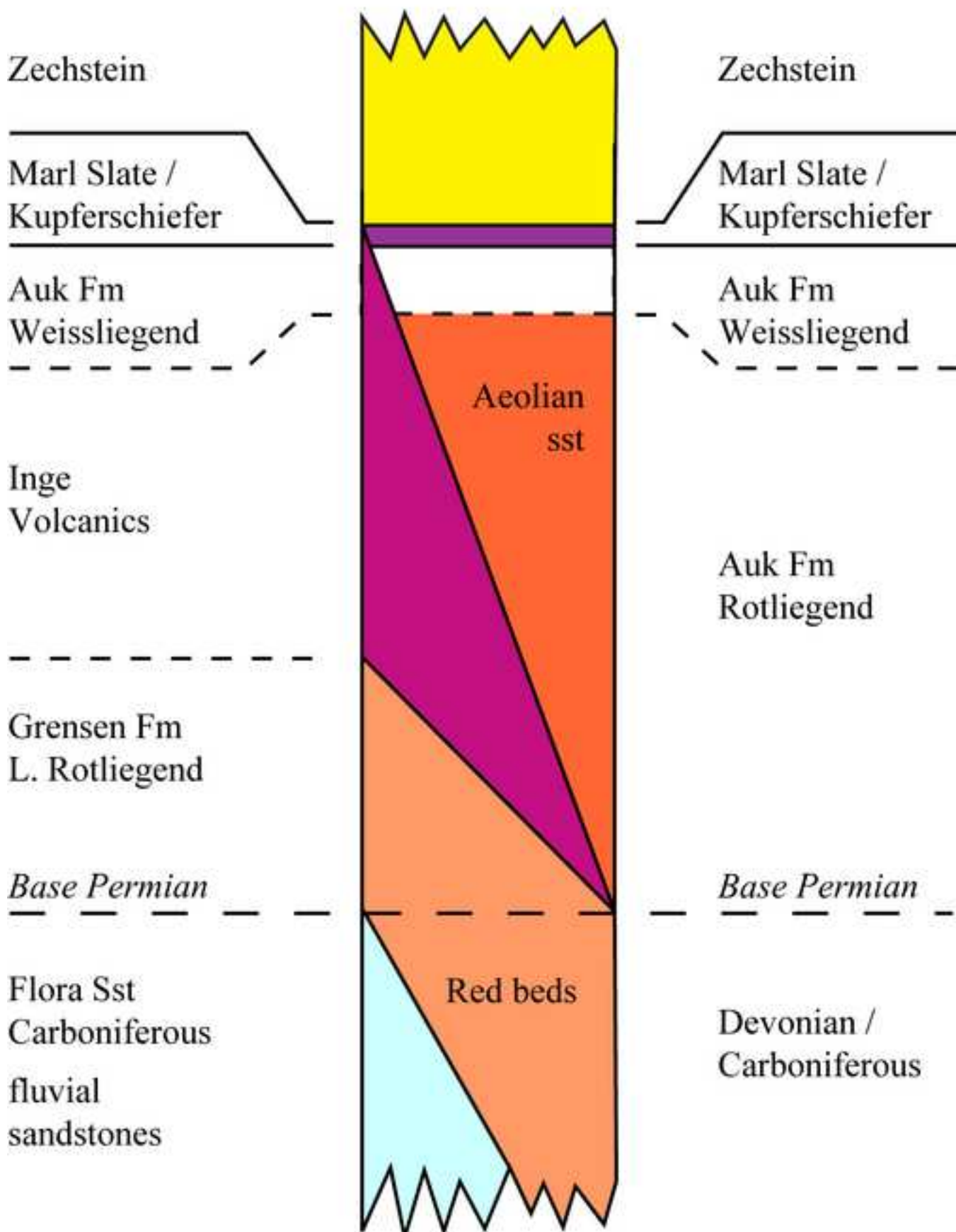


Figure 3
[Click here to download high resolution image](#)

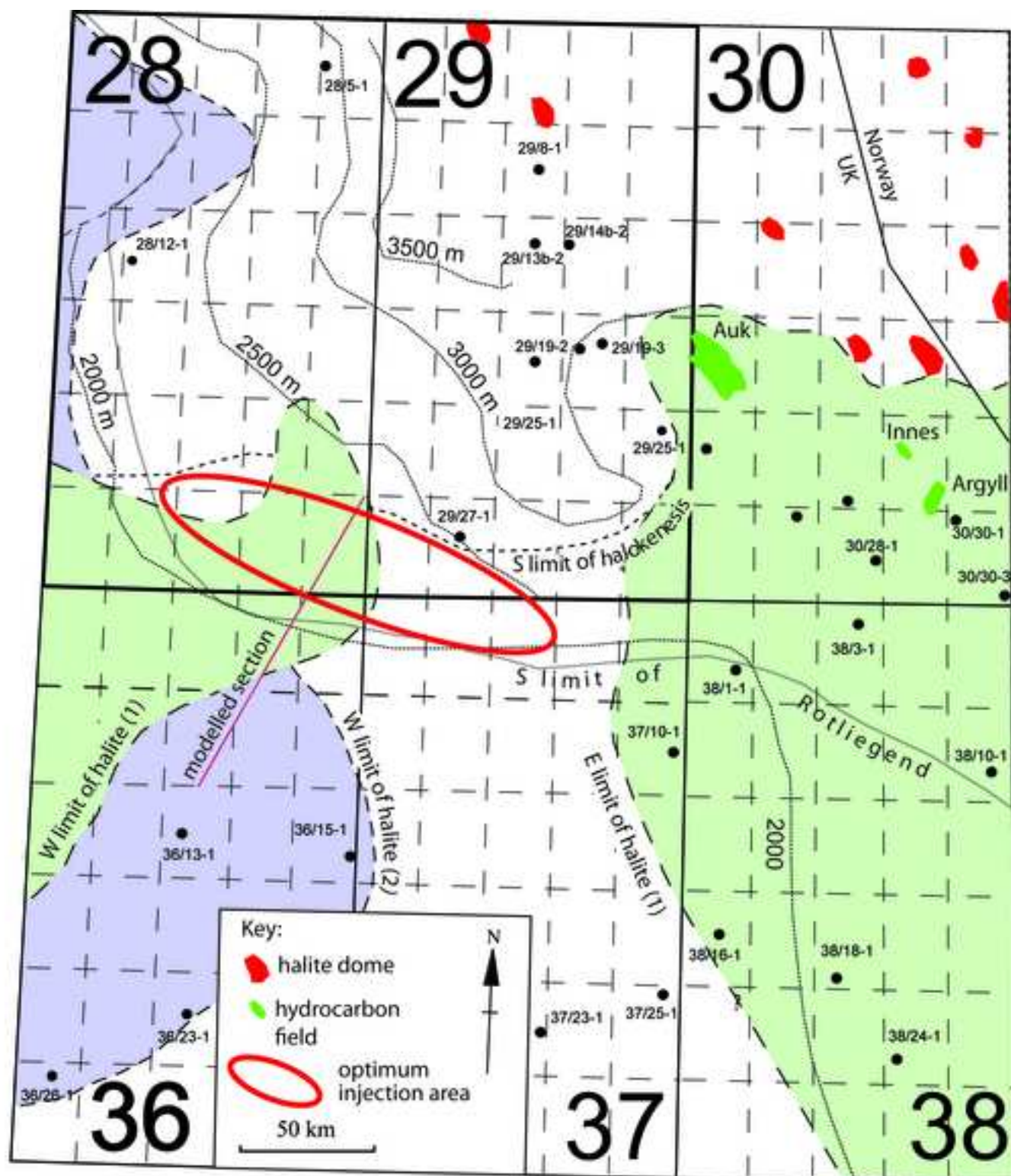


Figure 4

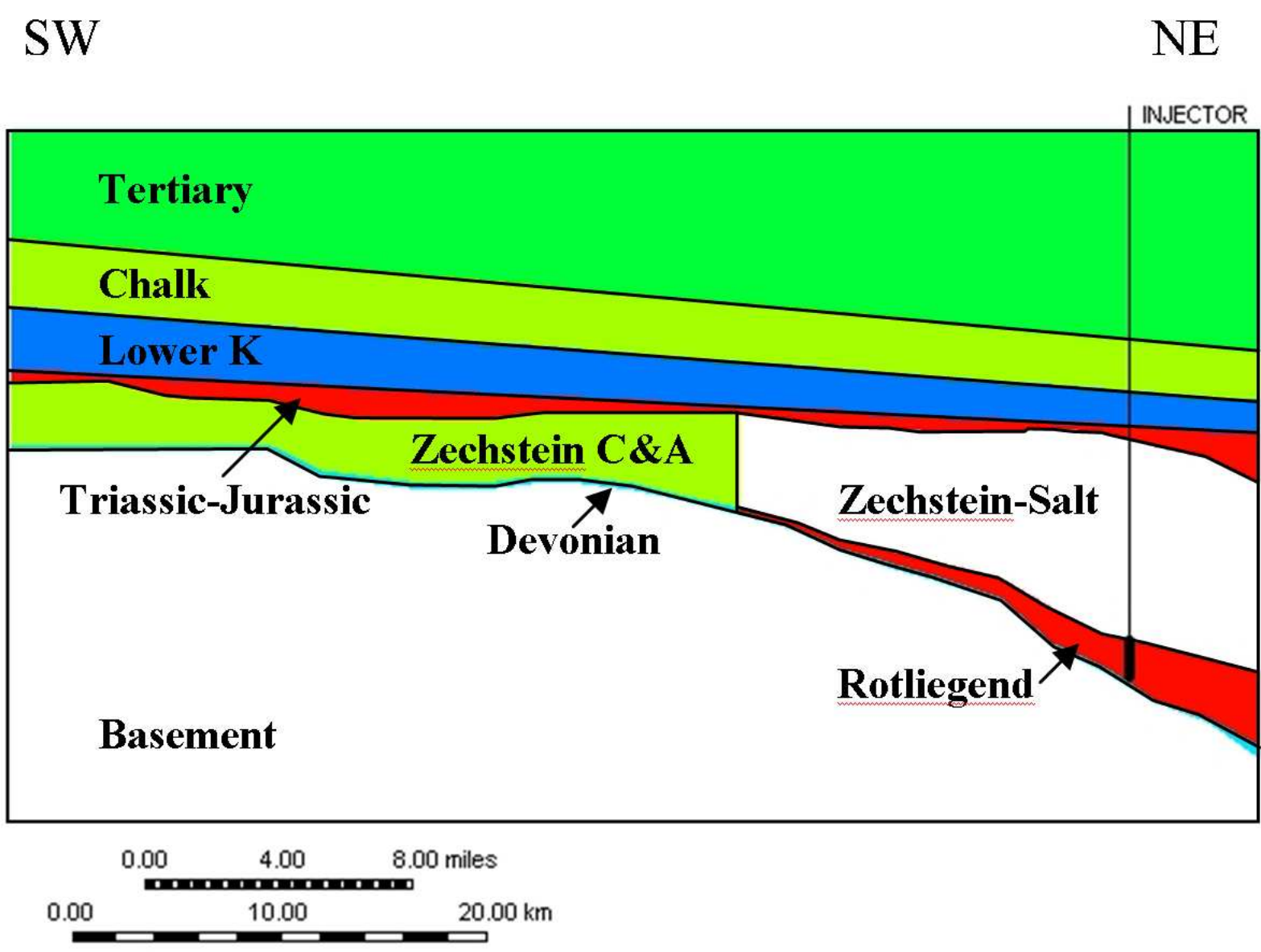


Figure 5
[Click here to download high resolution image](#)



Figure 6
[Click here to download high resolution image](#)

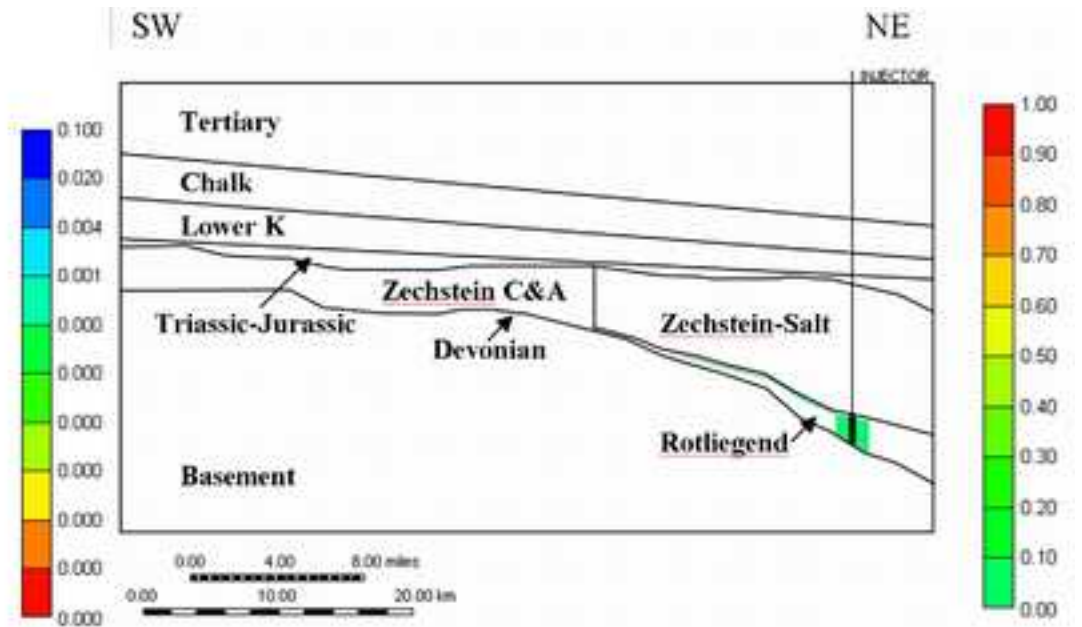
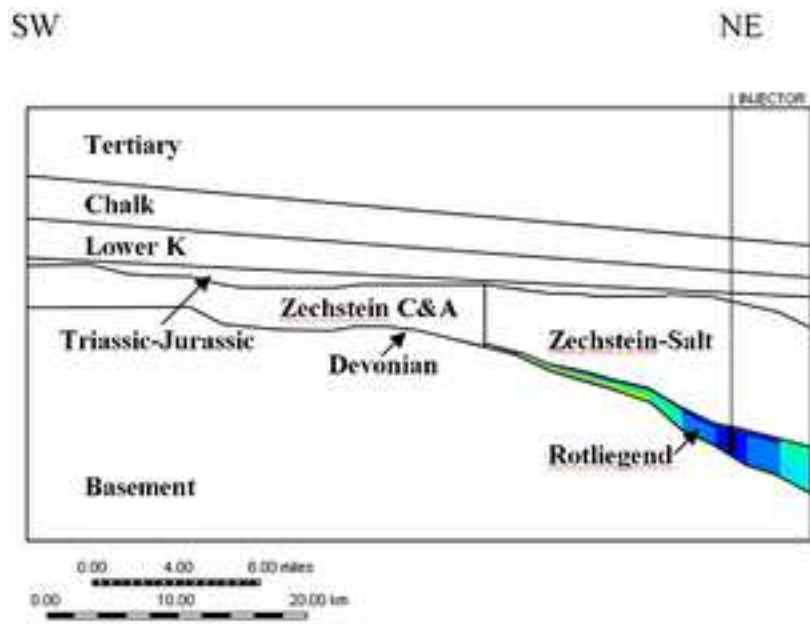


Figure 7
[Click here to download high resolution image](#)

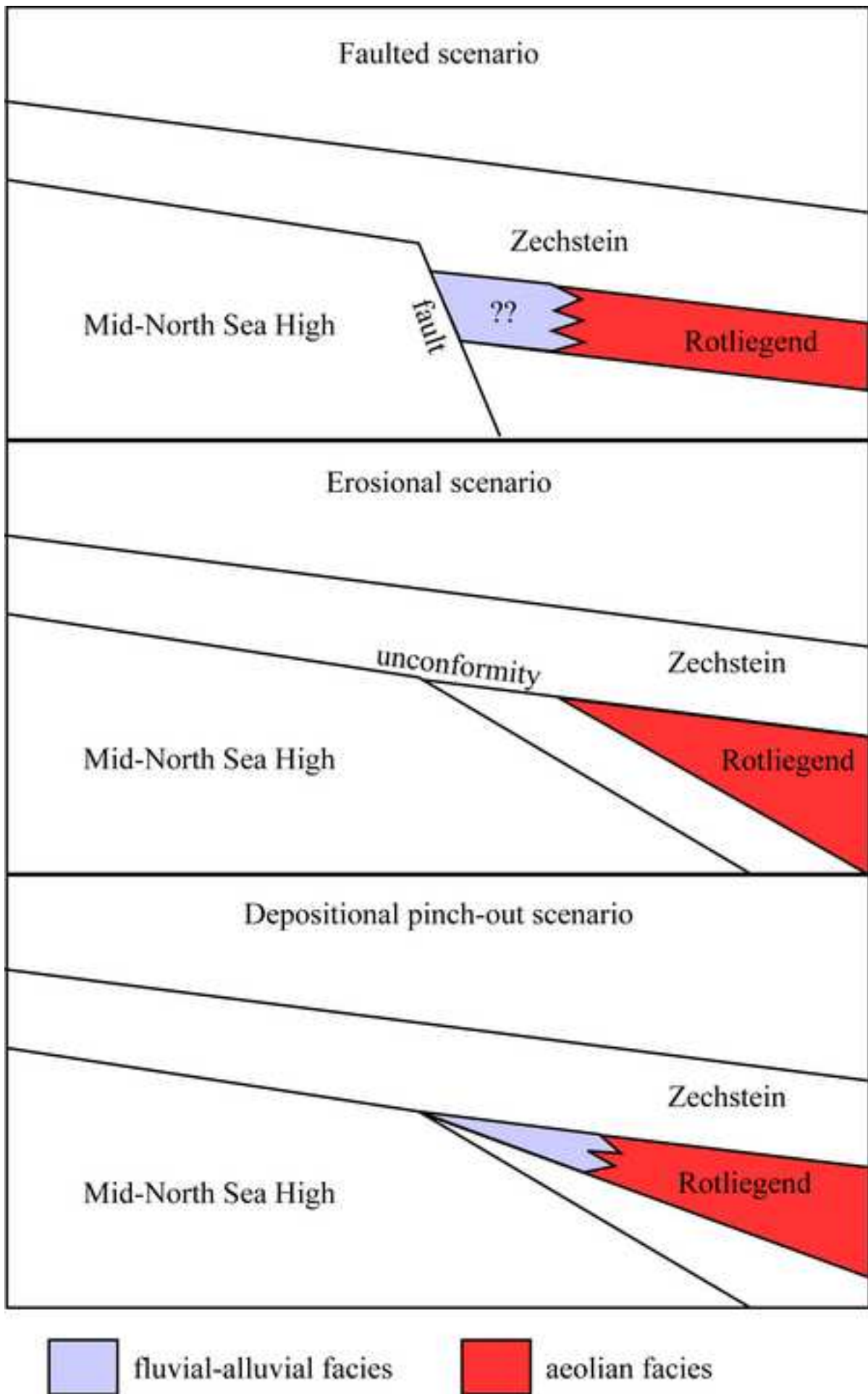


Figure 8
[Click here to download high resolution image](#)

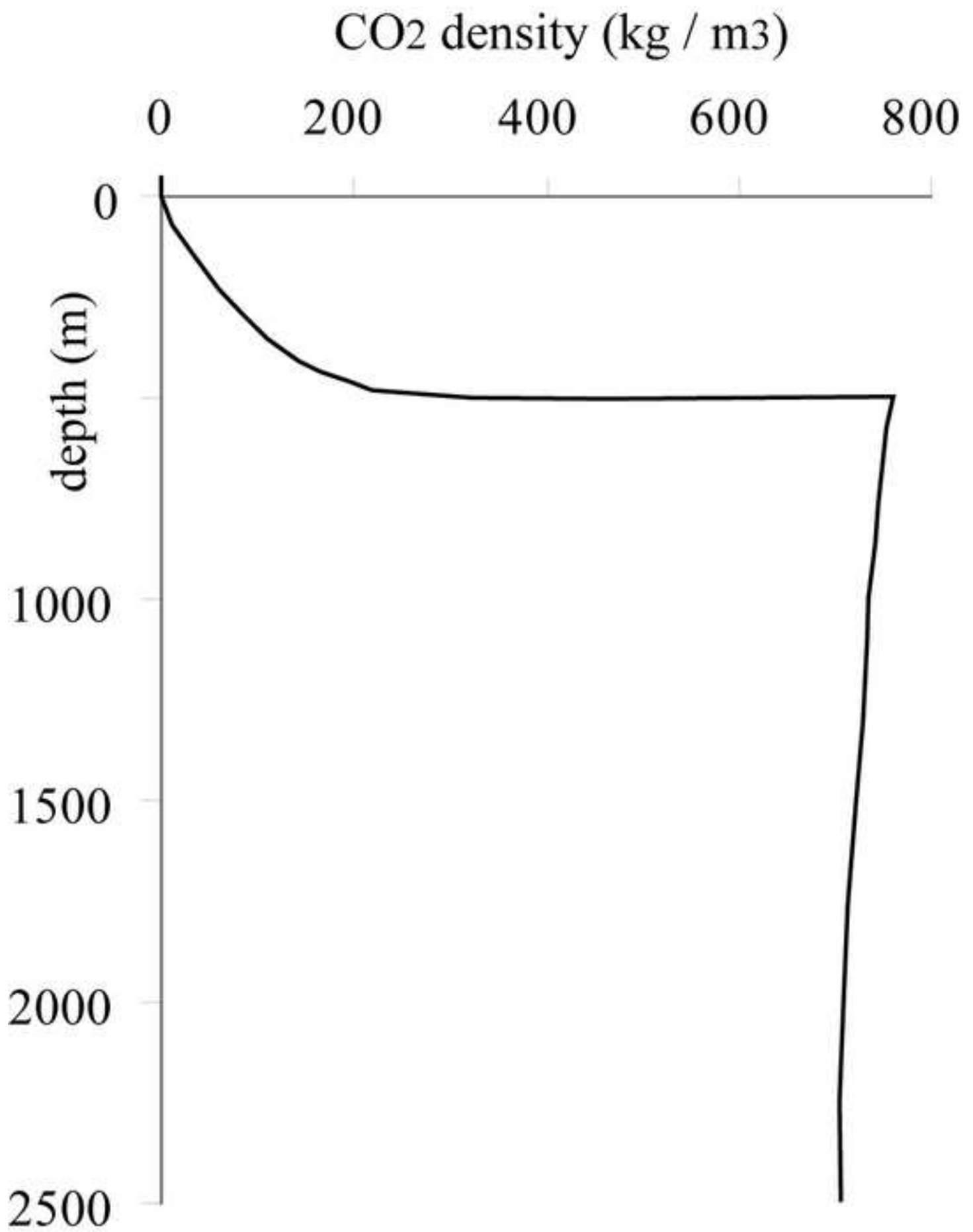


Figure 9

[Click here to download high resolution image](#)

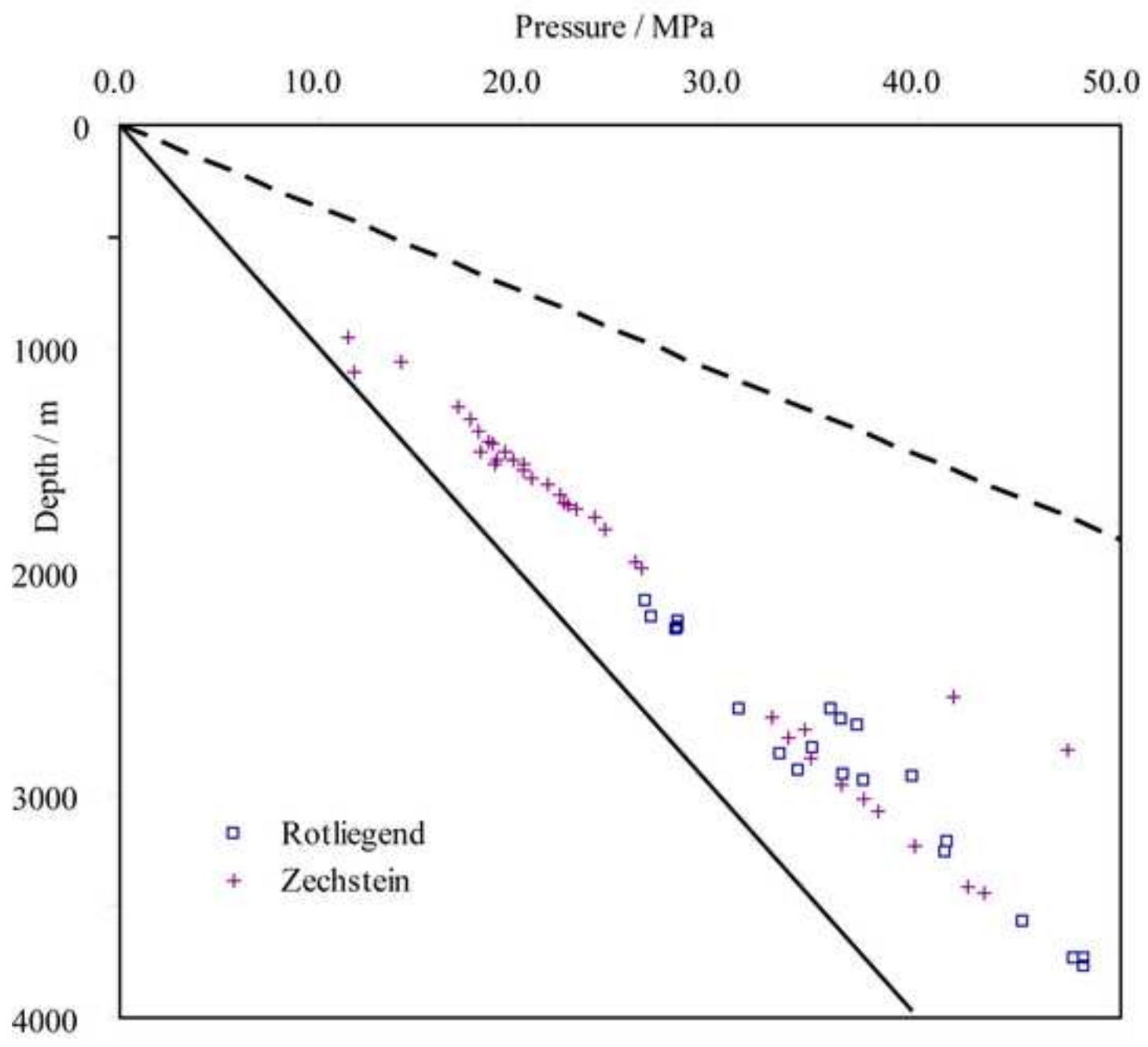
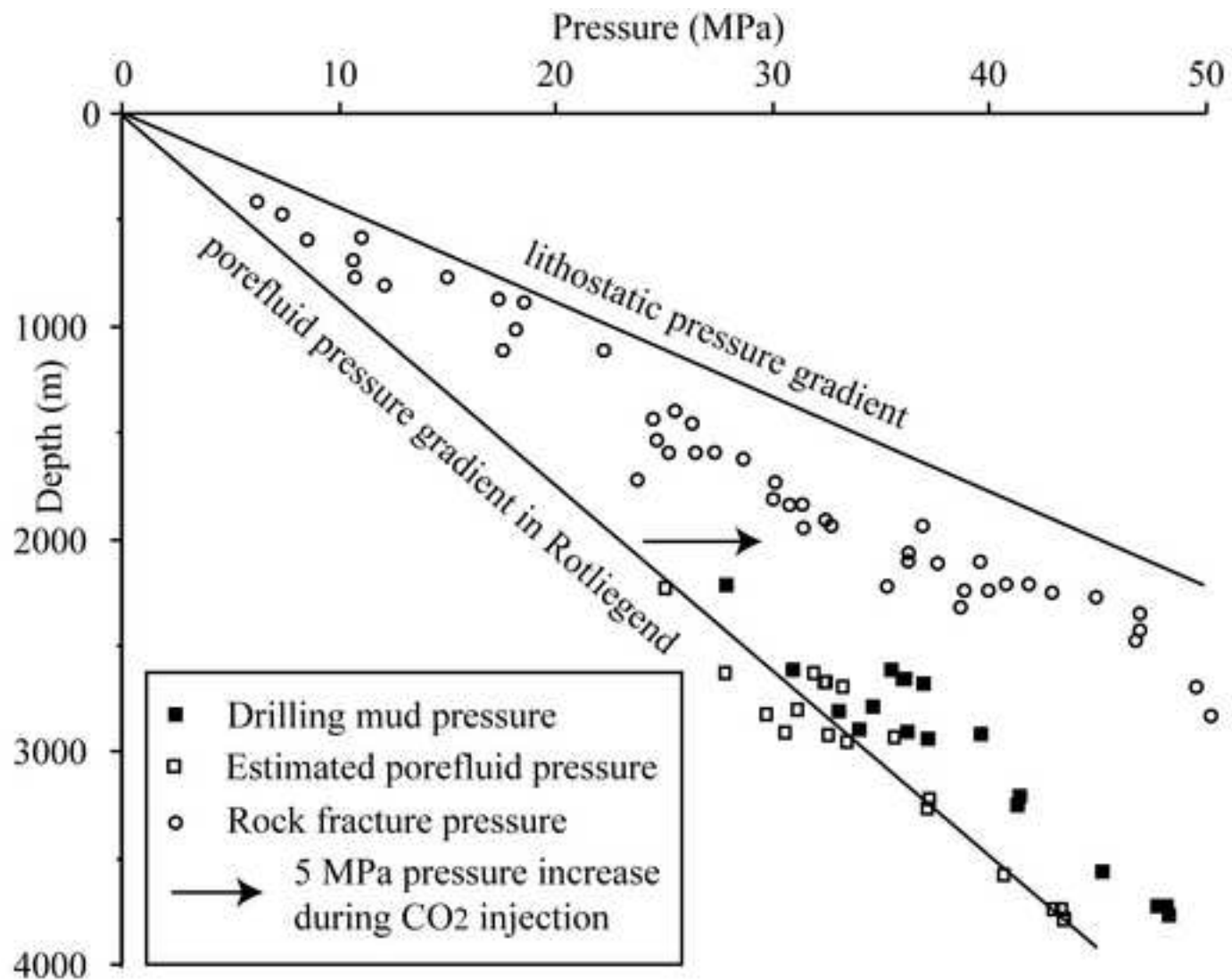


Figure 10

[Click here to download high resolution image](#)



Wilkinson et al. Fig 3, fracture pressures from Gaarenstroom et al., 1993, *Petrol Geol of NW Europe* 4, p1308

Figure 11

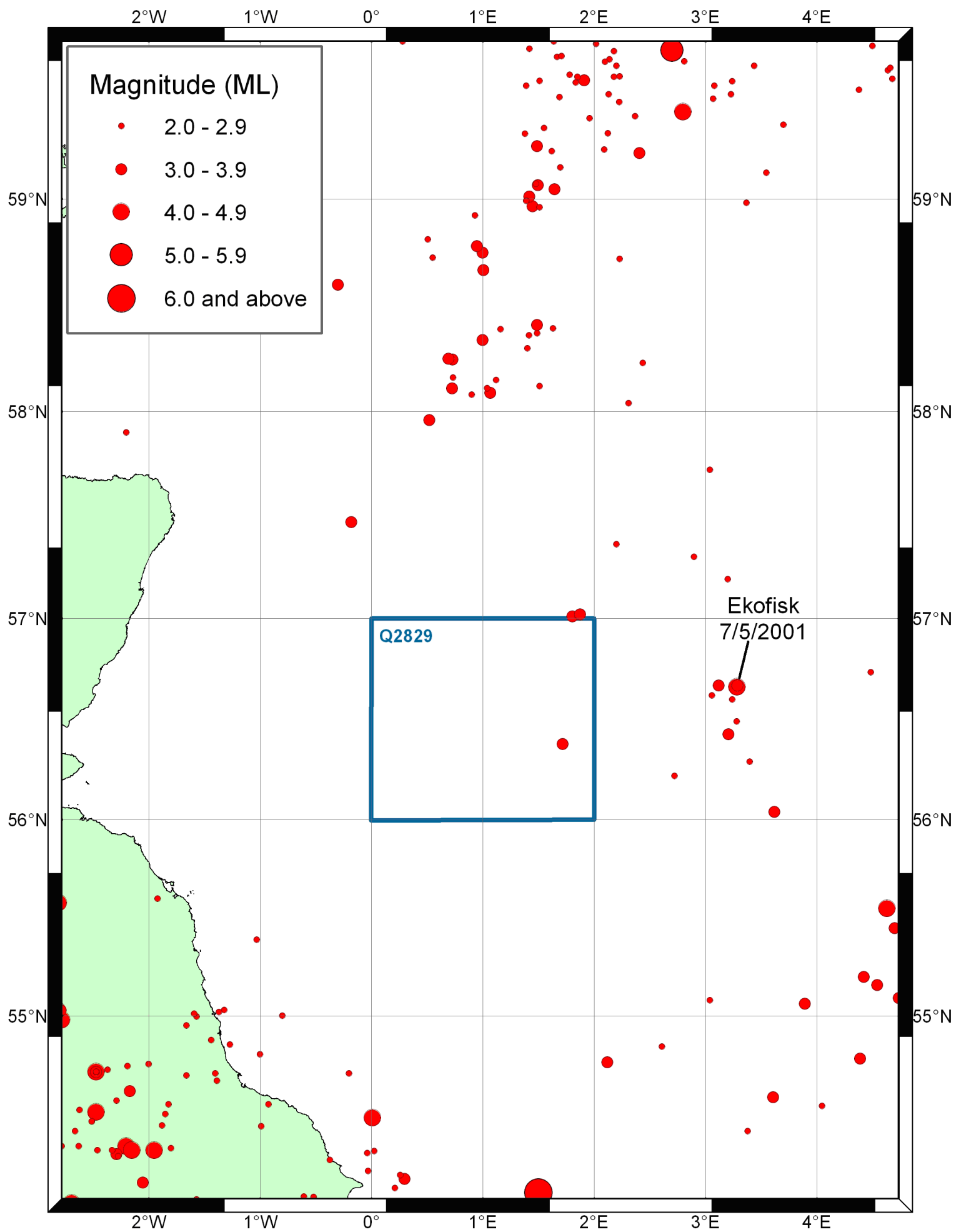


Figure 12
[Click here to download high resolution image](#)

